

Syntheses and Vibrational and ^{13}C MAS-NMR Spectra of Bis(carbonyl)mercury(II) Undecafluorodiantimonate(V) ($[\text{Hg}(\text{CO})_2][\text{Sb}_2\text{F}_{11}]_2$) and of Bis(carbonyl)dimercury(I) Undecafluorodiantimonate ($[\text{Hg}_2(\text{CO})_2][\text{Sb}_2\text{F}_{11}]_2$) and the Molecular Structure of $[\text{Hg}(\text{CO})_2][\text{Sb}_2\text{F}_{11}]_2$

M. Bodenbinder,[†] G. Balzer-Jöllenbeck,[†] H. Willner,^{*,†} R. J. Batchelor,[‡] F. W. B. Einstein,[‡] C. Wang,[§] and F. Aubke^{*,§}

Institut für Anorganische Chemie der Universität, Callinstrasse 9, D-30167 Hannover, Germany, Department of Chemistry, Simon Fraser University, Burnaby, British Columbia V5A 1S6, Canada, and Department of Chemistry, The University of British Columbia, Vancouver, British Columbia V6T 1Z1, Canada

Received June 7, 1995[⊗]

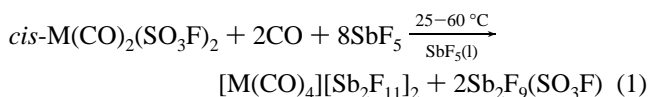
The synthesis of bis(carbonyl)mercury(II) undecafluorodiantimonate(V), $[\text{Hg}(\text{CO})_2][\text{Sb}_2\text{F}_{11}]_2$, and that of the corresponding mercury(I) salt $[\text{Hg}_2(\text{CO})_2][\text{Sb}_2\text{F}_{11}]_2$ are accomplished by the solvolyses of $\text{Hg}(\text{SO}_3\text{F})_2$ or of Hg_2F_2 , treated with fluorosulfuric acid, HSO_3F , in liquid antimony(V) fluoride at 80 or 60 °C, respectively, in an atmosphere of CO (500–800 mbar). The resulting white solids are the first examples of metal carbonyl derivatives formed by a post-transition element. Both salts are characterized by FT-IR, FT-Raman, and ^{13}C -MAS-NMR spectroscopy. For $[\text{Hg}(\text{CO})_2][\text{Sb}_2\text{F}_{11}]_2$, unprecedentedly high CO stretching frequencies ($\bar{\nu}_{\text{av}} = 2279.5 \text{ cm}^{-1}$) and stretching force constant ($f_r = 21.0 \pm 0.1 \times 10^2 \text{ Nm}^{-1}$) are obtained. Equally unprecedented is the $^1J(^{13}\text{C}-^{199}\text{Hg})$ value of $5219 \pm 5 \text{ Hz}$ observed in the ^{13}C MAS-NMR spectrum of the ^{13}C labeled isotopomers at $\delta = 168.8 \pm 0.1 \text{ ppm}$. The corresponding values ($\bar{\nu}_{\text{av}} = 2247 \text{ cm}^{-1}$, $f_r = (20.4 \pm 0.1) \times 10^2 \text{ Nm}^{-1}$, $^1J(^{13}\text{C}-^{199}\text{Hg}) = 3350 \pm 50 \text{ Hz}$ and $^2J(^{13}\text{C}-^{199}\text{Hg}) 850 \pm 50 \text{ Hz}$) are found for $[\text{Hg}_2(\text{CO})_2][\text{Sb}_2\text{F}_{11}]_2$, which has lower thermal stability (decomposition point in a sealed tube is 140 °C vs 160 °C for the Hg(II) compound) and a decomposition pressure of 8 Torr at 20 °C. The mercury(I) salt is sensitive toward oxidation to $[\text{Hg}(\text{CO})_2][\text{Sb}_2\text{F}_{11}]_2$ during synthesis. Both linear cations (point group $D_{\infty h}$) are excellent examples of nonclassical (σ -only) metal–CO bonding. Crystal data for $[\text{Hg}(\text{CO})_2][\text{Sb}_2\text{F}_{11}]_2$: monoclinic, space group $P2_1/n$; $Z = 2$; $a = 7.607(2) \text{ \AA}$; $b = 14.001(3) \text{ \AA}$; $c = 9.730(2) \text{ \AA}$; $\beta = 111.05(2)^\circ$; $V = 967.1 \text{ \AA}^3$; $T = 195 \text{ K}$; $R_F = 0.035$ for 1983 data ($I_0 \geq 2.5\sigma(I_0)$) and 143 variables. The Hg atom lies on a crystallographic inversion center. The Hg–C–O angle is $177.7(7)^\circ$. The length of the mercury–carbon bond is $2.083(10) \text{ \AA}$ and of the C–O bond $1.104(12) \text{ \AA}$ respectively. The structure is stabilized in the solid state by a number of significant secondary interionic Hg–F and C–F contacts.

Introduction

Recent studies by Strauss^{1,2} and his group, by Adelhalm et al.,^{3b} and by us^{3a–9} have focused attention on a group of carbonyl derivatives of the noble metals, that differ in all important aspects from the well-known “classical” transition metal carbonyls.^{10–12} This group of “nonclassical” metal carbonyls

consists of the binary cations $[\text{Ag}(\text{CO})]^+$,¹ $[\text{Au}(\text{CO})]^+$,⁴ $[\text{Ag}(\text{CO})_2]^{2+}$,² $[\text{Au}(\text{CO})_2]^{+,3,4}$ $[\text{Ag}(\text{CO})_3]^+$,^{2b} $\text{cyclo}[\text{Pd}_2(\mu\text{-CO})_2]^{2+,8}$ $[\text{Pd}(\text{CO})_4]^{2+,5}$ and $[\text{Pt}(\text{CO})_4]^{2+,5,7}$ which may be generated and studied in strong protonic acids like HSO_3F ^{3a–5,7} or anhydrous HF,^{3b} in superacids like magic acid⁴ or $\text{HSO}_3\text{F}\text{-SbF}_5$, or in strong Lewis acids such as liquid SbF_5 .^{4,5}

In the solid state, the nonclassical carbonyl cations are stabilized by very weakly nucleophilic anions like $[\text{B}(\text{OTeF}_5)_4]^{-,1,2}$ $[\text{Pt}(\text{SO}_3\text{F})_6]^{2-,7}$ $[\text{UF}_6]^{-,3b}$ $\text{SO}_3\text{F}^{-,8}$ and $[\text{Sb}_2\text{F}_{11}]^{-,4,5}$ or by monodentate fluorosulfate groups in covalent, cationic derivatives such as $\text{Au}(\text{CO})\text{SO}_3\text{F}$ ^{3a} or $\text{cis-M}(\text{CO})_2(\text{SO}_3\text{F})_2$, $\text{M} = \text{Pd}$ or Pt .^{6,9} As shown by the solvolysis reaction⁵ ($\text{M} = \text{Pd}$ or Pt),



the carbonyl fluorosulfates^{3a,9} serve as precursors to the metal carbonyl fluoroantimonates. Neither the highly acidic reaction media nor the fluoroanions, which rank among the weakest nucleophiles,¹³ have previously played a significant role in the

- * Authors to whom correspondence should be addressed.
[†] Institut für Anorganische Chemie der Universität.
[‡] Simon Fraser University.
[§] The University of British Columbia.
[⊗] Abstract published in *Advance ACS Abstracts*, November 15, 1995.
 (1) Hurlburt, P. K.; Anderson, O. P.; Strauss, S. H. *J. Am. Chem. Soc.* **1991**, *113*, 6277.
 (2) (a) Hurlburt, P. K.; Rack, J. J.; Dec, S. F.; Anderson, O. P.; Strauss, S. H. *Inorg. Chem.* **1993**, *32*, 373. (b) Rack, J. J.; Moasser, B.; Gargulak, J. D.; Gladfelter, W. L.; Hochheimer, H. D.; Strauss, S. H. *J. Chem. Soc., Chem. Commun.* **1994**, 685.
 (3) (a) Willner, H.; Aubke, F. *Inorg. Chem.* **1990**, *29*, 2195. (b) Adelhalm, M.; Bacher, W.; Höhn, E. G.; Jacob, E. *Chem. Ber.* **1991**, *124*, 1559.
 (4) Willner, H.; Schaebs, J.; Hwang, G.; Mistry, F.; Jones, R.; Trotter, J.; Aubke, F. *J. Am. Chem. Soc.* **1992**, *114*, 8972.
 (5) Hwang, G.; Wang, C.; Aubke, F.; Bodenbinder, M.; Willner, H. *Can. J. Chem.* **1993**, *71*, 1532.
 (6) Hwang, G.; Wang, C.; Bodenbinder, M.; Willner, H.; Aubke, F. *J. Fluorine Chem.* **1994**, *66*, 159.
 (7) Hwang, G.; Bodenbinder, M.; Willner, H.; Aubke, F. *Inorg. Chem.* **1993**, *32*, 4667.
 (8) Wang, C.; Bodenbinder, M.; Willner, H.; Rettig, S.; Trotter, J.; Aubke, F. *Inorg. Chem.* **1994**, *33*, 779.
 (9) Wang, C.; Willner, H.; Bodenbinder, M.; Batchelor, R. J.; Einstein, F. W. B.; Aubke, F. *Inorg. Chem.* **1994**, *33*, 3521.

- (10) Cotton, F. A.; Wilkinson, G. *Advanced Inorganic Chemistry*, 5th ed.; Wiley: New York, NY, 1988; pp 58 and 1035.
 (11) Pruchnick, F. P. *Organometallic Chemistry of Transition Elements*; Plenum Press: New York, NY, 1990; p 23.
 (12) Werner, H. *Angew. Chem., Int. Ed. Engl.* **1990**, *29*, 1109.

synthesis and stabilization of classical transition metal carbonyl derivatives.^{10–12}

It is known, for some time now, that neutral binary carbonyl fragments of the types $M(\text{CO})_n$, $M = \text{Pd, Pt, Ag, or Au}$, with n ranging from 1 up to 4, form in metal atom reactions with CO and are studied under matrix isolation conditions.¹⁴ The nonclassical carbonyl cations are, with the exception of the silver salts, thermally stable beyond 100 °C.

The geometries, linear for $[\text{M}(\text{CO})_2]^+$, $M = \text{Ag}^2$ and Au ,^{3,4} and square planar for $[\text{M}(\text{CO})_4]^{2+}$, $M = \text{Pd}^5$ and Pt ,^{5,7} are unprecedented in classical binary metal carbonyl species^{10,12} where so far only octahedral cations of the type $[\text{M}(\text{CO})_6]^+$, $M = \text{Mn, Tc, or Re}$ are known.¹⁵

Vibrational spectroscopy, which has been very useful in the study and structural characterization of classical transition metal carbonyl compounds,^{16,17} reveals the most striking feature of the nonclassical noble metal carbonyl cations: The CO stretching frequencies $\bar{\nu}(\text{CO})$ and f_r , the stretching force constants, are raised significantly rather than lowered relative to $\bar{\nu}(\text{CO})$ of 2143 cm^{-1} and f_r of $18.6 \times 10^2 \text{ Nm}^{-1}$ in gaseous CO.¹⁸ Average values as high as 2260 cm^{-1} for $\bar{\nu}(\text{CO})$ and f_r values of $20.6 \times 10^2 \text{ Nm}^{-1}$ have been reported for $[\text{M}(\text{CO})_4]^{2+}$ $M = \text{Pd}^5$ or Pt^5 . The usual range for terminal CO ligands is $\bar{\nu}$ 2125–1850 cm^{-1} .^{10,16,17}

In ¹³C NMR spectra of nonclassical carbonyl compounds, chemical shifts of 175–140 ppm have been observed,^{2,4,7,8} with resonances at lower frequencies than found for CO (184 ppm in HSO_3F).⁴ Classical metal carbonyls have ¹³C chemical shifts usually between 190 and 220 ppm.¹⁹

The results, summarized briefly above, allow two conclusions regarding structure and bonding in nonclassical noble metal carbonyl cations: (i) π -back-bonding, an essential component of metal–CO bonding in classical transition metal carbonyls, appears to be reduced to insignificance, and (ii) the noble gas formalism (rule of eighteen), generally valid for binary metal carbonyls, is irrelevant: $[\text{M}(\text{CO})_2]^+$, $M = \text{Ag or Au}$, have 14 and $[\text{M}(\text{CO})_4]^{2+}$, $M = \text{Pd or Pt}$, have 16 valence electrons associated with the central metal ion. The coordination numbers and geometries, two and linear for gold(I)²⁰ and four and square planar for Pd(II)²¹ or Pt(II),²² are commonly found in coordination compounds of the d^{10} or d^8 metal ions with σ donor ligands.^{20,22}

Since carbon monoxide, CO, and the cyanide anion, CN^- , are isoelectronic, it is not surprising that the noble metal carbonyl cations show very strong similarities in their structural, spectroscopic, and bonding features to those of the correspond-

ing, isoelectronic coordination complexes with cyanide, CN^- , as ligand.^{23,24} This analogy relates $[\text{Ag}(\text{CO})_2]^+$ to $[\text{Ag}(\text{CN})_2]^-$, $[\text{Au}(\text{CO})_2]^+$ to $[\text{Au}(\text{CN})_2]^-$ or $\text{Hg}(\text{CN})_2$, and $[\text{M}(\text{CO})_4]^{2+}$ to $[\text{M}(\text{CN})_4]^{2-}$, $M = \text{Pd or Pt}$, or to $[\text{Au}(\text{CN})_4]^-$.

For the cyanide complexes, extensive structural studies^{23,24} and detailed vibrational analyses^{25,26} exist, including normal coordinate analyses and force field calculations. These studies suggest substantially reduced $M \rightarrow \text{CN}$ π -back-bonding, which results in raised $\bar{\nu}(\text{CN})$ and f_r values relative to the free CN^- .^{18c,25,26} In addition, the noble gas formalism is not applicable to the coordination complexes of CN^- with electron rich metals. These observations allow the conclusion that thermally stable, isoelectronic carbonyl cations of main-group and post-transition metals should be obtainable in highly acidic media or solid compounds.

The bis(carbonyl)mercury(II) cation $[\text{Hg}(\text{CO})_2]^{2+}$ becomes an obvious choice as the object of synthetic attempts for the following reasons: (i) The isoelectronic $[\text{Au}(\text{CO})_2]^+$ cation is easily formed in solutions of $\text{HSO}_3\text{F}^{3a}$ or SbF_5 .⁴ (ii) Its salt with $[\text{Sb}_2\text{F}_{11}]^-$ as counteranion has considerably higher thermal stability (dec pt 156 °C)⁴ than $[\text{Ag}(\text{CO})_2][\text{B}(\text{OTeF}_5)_4]^{2-}$ or $[\text{Au}(\text{CO})_2][\text{UF}_6]^{2-}$.^{3b} (iii) Even though the molecular structure of $[\text{Au}(\text{CO})_2][\text{Sb}_2\text{F}_{11}]$ has so far not been solved, the reported complete vibrational spectrum of the linear molecule ($D_{\infty h}$) and its ¹³C and ¹⁸O isotopomers, normal coordinate analysis, and valence force field calculations⁴ should allow a meaningful comparison to $[\text{Hg}(\text{CO})_2]^{2+}$. (iv) For the neutral, isoelectronic molecule $\text{Hg}(\text{CN})_2$, both precise vibrational information^{25,27} and the molecular structure, obtained by X-ray and neutron diffraction,²⁸ are known. (v) Finally, ¹³C NMR should provide for $[\text{Hg}(\text{CO})_2]^{2+}$ not only chemical shift information which may be compared to previous work^{2,4,18} but also ¹ $J(^{13}\text{C}-^{199}\text{Hg})$ coupling constants, that should permit comparison to related work in this area.²⁹

In summary, suitable reaction media, a promising synthetic route, and well characterized isoelectronic analogous molecules are known and provide indications that $[\text{Hg}(\text{CO})_2]^{2+}$ should be obtainable.

We want to report here on the synthesis of bis(carbonyl)-mercury(II) undecafluorodiantimonate(V), $[\text{Hg}(\text{CO})_2][\text{Sb}_2\text{F}_{11}]_2$, to our knowledge the first example of a thermally stable carbonyl derivative of a post-transition metal. The compound is characterized by microanalysis, its vibrational spectra, the ¹³C NMR-MAS spectrum, obtained for the ¹³C labeled isotopomer, and its molecular structure, determined by single crystal X-ray diffraction at 195 K.

Also reported here are the synthesis, vibrational spectra, and the ¹³C NMR-MAS spectrum of the related mercurous compound $[\text{Hg}_2(\text{CO})_2][\text{Sb}_2\text{F}_{11}]_2$. The cream colored solid shows lower thermal stability than the Hg(II) compound and is characterized by spectroscopic means. A preliminary account of the syntheses of $[\text{Hg}(\text{CO})_2][\text{Sb}_2\text{F}_{11}]_2$ and of $[\text{Hg}_2(\text{CO})_2][\text{Sb}_2\text{F}_{11}]_2$, their partial vibrational spectra (CO stretching region only), and their ¹³C NMR-MAS spectra has appeared recently in a preliminary communication.³⁰

- (13) Mallela, S. P.; Yap, S.; Sams, J. R.; Aubke, F. *Inorg. Chem.* **1986**, *25*, 4327.
- (14) Moskovits, M.; Ozin, G. A. *Cryochemistry*; John Wiley and Sons: New York, 1976; p 261, and references therein.
- (15) Abel, E. W.; Tyfield, S. P. *Adv. Organomet. Chem.* **1970**, *8*, 117.
- (16) Braterman, P. S. *Metal Carbonyl Spectra*; Academic Press: New York, NY, 1975.
- (17) Kettle, S. F. A. *Top. Curr. Chem.* **1977**, *71*, 111.
- (18) (a) Browning, J.; Goggin, P. L.; Goodfellow, R. J.; Norton, M. J.; Rattray, A. J. M.; Taylor, B. F.; Mink, J. *J. Chem. Soc., Dalton Trans.* **1977**, 2061. (b) Nakamoto, K. *Infrared Spectra of Inorganic and Coordination Compounds*, 2nd ed.; John Wiley and Sons: New York, NY, 1970; p 78. (c) Field, G. R.; Sherman, W. F. *J. Chem. Phys.* **1967**, *47*, 2378.
- (19) Mann, B. E. *Adv. Organomet. Chem.* **1974**, *12*, 133.
- (20) (a) Puddephatt, R. J. *The Chemistry of Gold*; Elsevier: Amsterdam, 1978. (b) Puddephatt, R. J. *Comprehensive Coordination Chemistry*; Wilkinson, G., Ed.; Pergamon Press: Oxford, U.K., 1987; Vol. 5, p 861.
- (21) Barnard, C. F. J.; Russel, M. J. H. In *Comprehensive Coordination Chemistry*; Wilkinson, G., Ed.; Pergamon Press: Oxford, U.K., 1987; Vol. 5, p 1099.
- (22) Roundhill, D. M. In *Comprehensive Coordination Chemistry*; Wilkinson, G., Ed.; Pergamon Press: Oxford, U.K., 1987; Vol. 5, p 351.

- (23) Chadwick, B. M.; Sharpe, A. G. *Adv. Inorg. Chem. Radiochem.* **1966**, *8*, 83.
- (24) Sharpe, A. G. *The Chemistry of Cyano Complexes of Transition Metals*; Academic Press: New York, 1976.
- (25) Jones, L. H. *Inorganic Vibrational Spectroscopy*; Marcel Dekker: New York, 1971; Vol. 1, p 122 and references therein.
- (26) Kubas, G. J.; Jones, L. H. *Inorg. Chem.* **1974**, *13*, 2816.
- (27) Jones, L. H. *J. Chem. Phys.* **1966**, *44*, 3643.
- (28) (a) Hvorslef, J. *Acta Chem. Scand.* **1958**, *12*, 1568. (b) Secombe, R. C.; Kennard, C. H. L. *J. Organomet. Chem.* **1969**, *18*, 243.
- (29) (a) Sebald, A.; Wrackmeyer, B. *Spectrochim. Acta, A* **1982**, *38*, 163. (b) Sebald, A.; Wrackmeyer, B. *J. Magn. Reson.* **1985**, *63*, 397.

Experimental Section

(a) Chemicals. Doubly distilled mercury (Riedel deHaen), mercurous fluoride Hg_2F_2 technical grade (Aldrich Chemicals), and ^{13}C O (99% pure, IC Chemicals) were obtained from commercial sources and used without further purification. Carbon monoxide with a normal isotope distribution is obtained from Linde Gas. Fluorosulfuric acid, HSO_3F (technical), and perfluorobutyl sulfuryl fluoride, $\text{C}_4\text{F}_9\text{SO}_2\text{F}$, were kindly supplied by Bayer A.G., Leverkusen, Germany. Technical grade HSO_3F was purified by double distillation at atmospheric pressure following a published procedure.³¹ Bis(fluorosulfuryl) peroxide, $\text{S}_2\text{O}_6\text{F}_2$, was obtained by catalytic fluorination of sulfur trioxide.³² Mercuric fluorosulfate, $\text{Hg}(\text{SO}_3\text{F})_2$, is synthesized by oxidation of mercury with $\text{S}_2\text{O}_6\text{F}_2$ in HSO_3F as reported previously.³³ Antimony(V) fluoride (Bayer, A.G.; Merck, Darmstadt, or Atochem North America, formerly Ozark-Mahoning) was purified by distillation at atmospheric pressure followed by trap to trap distillation *in vacuo* in a borosilicate apparatus.

(b) Instrumentation. Infrared spectra were recorded on a Bruker IFS-66v instrument, with a range of $4000\text{--}50\text{ cm}^{-1}$ (University of Hannover), and a Bomen MB-102 instrument, with a range of $4000\text{--}400\text{ cm}^{-1}$ (UBC).

FT-Raman spectra were recorded with Bruker FRA-106FT Raman accessory mounted on an optical bench of the IFS-66v instrument. Raman samples were contained in melting point capillaries. Infrared samples were crushed between AgBr (Harshaw Chemicals) or polyethylene discs.

^{13}C NMR spectra were obtained on a Bruker MSL-200 FT spectrometer operating at 50.322 MHz. Liquid samples were contained in tubes of 5 mm o.d. fitted with rotationally symmetrical Teflon stem valves (Young, London, U.K.) and placed in the center of 10 mm o.d. tubes. CDCl_3 , used as lock and as external reference, was added to the outer tube.

Solid-state ^{13}C NMR spectra (MAS) were recorded using a broad band probe, MAS DLK, 39–82 MHz (Bruker), with rotational frequencies between 2000 and 4800 Hz. Parameters are as follows: frequency 50.322 MHz, resolution 6.1 Hz/point, time between pulses 10 s, pulse length 3.5 μs . Adamantane was used as standard (37.9 ppm).

Gaseous and volatile reagents and products were measured in a vacuum line of known volume. Pressure measurements were made with a Setra capacity manometer type 280E (Setra Instruments, Acton, MA). Synthetic reactions were carried out in various glass reactors (10–50 mL volume) fitted with Teflon stem valves (Young, London, U.K.) and Teflon-coated stirring bars. Solid materials were manipulated inside either an inert atmosphere box (Braun, Munich, Germany) filled with argon, with a residual moisture content of less than 0.1 ppm, or a Vacuum Atmosphere Corp. Drilab filled with dry N_2 as described before.^{3a} Solutions in $\text{HSO}_3\text{F}\text{--SbF}_5$ were prepared in an evacuable box (Mecaplex, Grenchen, Switzerland) filled with N_2 . Microanalyses were performed by either Beller Laboratories, Göttingen, Germany, or Mr. P. Borda, Department of Chemistry, UBC.

(c) Synthetic Reactions. A two part, V-shaped reaction vessel as shown in Figure 1 was used. Part A, equipped with a magnetic stirring bar, was employed as reactor, while part B was used in the sample isolation as described below in more detail.

(i) Synthesis of $[\text{Hg}(\text{CO})_2][\text{Sb}_2\text{F}_{11}]_2$. The reactor part A was filled with 212.7 mg (1.06 mmol) of Hg, and approximately 1 mL of $\text{S}_2\text{O}_6\text{F}_2$ and 2 mL of HSO_3F were transferred *in vacuo*. At room temperature, the reaction proceeded very quickly³³ and produced a white crystalline slurry. Removal of all volatiles *in vacuo* and subsequent drying of the reaction product produced 423 mg (1.06 mmol) of $\text{Hg}(\text{SO}_3\text{F})_2$. Subsequently, approximately 3 mL of SbF_5 was added by transfer *in vacuo*, and gaseous CO (pressure ~ 700 mbar) was admitted to the reactor. Heating of the mixture to $80\text{ }^\circ\text{C}$ converted SbF_5 to a mobile liquid, which allowed efficient stirring. The uptake of CO was accelerated by vigorous stirring and occasional shaking of the reactor. In the course of the reaction, a white crystalline slurry formed and

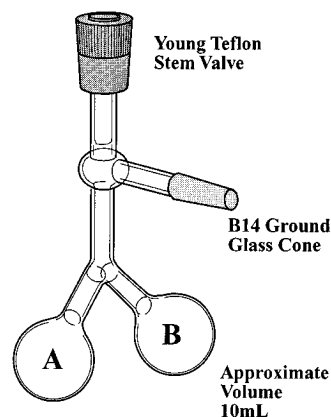


Figure 1. Reactor used for the synthesis of $[\text{Hg}(\text{CO})_2][\text{Sb}_2\text{F}_{11}]_2$ and $[\text{Hg}_2(\text{CO})_2][\text{Sb}_2\text{F}_{11}]_2$.

stirring became increasingly more difficult. After about 1 day, no further uptake of CO was noted, and the reactor was allowed to cool down to room temperature, while shaking was continued. Unreacted CO and most of the SbF_5 were removed *in vacuo*, and about 3 mL of $\text{C}_4\text{F}_9\text{SO}_2\text{F}$ was added *in vacuo* to the mixture, which dissolved the excess of SbF_5 but did not dissolve the white solid. Stirring of the mixture at room temperature produced a homogeneous suspension. When stirring was discontinued, a white crystalline solid had precipitated out. The clear, colorless supernatant was decanted into part B, and $\text{C}_4\text{F}_9\text{SO}_2\text{F}$ was condensed back onto the solid mass. The washing and decanting procedure was repeated three times. The product was dried by cooling part B to liquid nitrogen temperature. Subsequently, ampule A was flame-sealed and removed to an inert atmosphere box and opened there. A total of 1087 mg (0.936 mmol) of white crystalline material was obtained and identified as $[\text{Hg}(\text{CO})_2][\text{Sb}_2\text{F}_{11}]_2$ by microanalysis (see below). The yield of isolated product was 88% with losses due to the isolation procedure employed.

$[\text{Hg}(\text{CO})_2][\text{Sb}_2\text{F}_{11}]_2$ is a white crystalline hygroscopic solid that shrinks on heating at $140\text{ }^\circ\text{C}$ and melts under slow CO evolution at $160\text{ }^\circ\text{C}$. According to a Raman spectrum, the resolidified material has retained about 90% of the original CO contents. In contrast to $[\text{Au}(\text{CO})_2][\text{Sb}_2\text{F}_{11}]_2$,⁴ the white solid will dissolve in SO_2 and HSO_3F under CO evolution. In solution, the material is stable only in SbF_5 and magic acid ($\text{HSO}_3\text{F}\text{--SbF}_5$). The latter solvent is used to obtain single crystals.

Anal. Calcd for $\text{C}_2\text{O}_2\text{F}_{22}\text{HgSb}_4$: C, 2.1; Sb, 41.9; F, 36.0. Found: C, 1.9; Sb, 42.3; F, 35.5. Attempts to analyze for mercury gave an extremely low value of 9.6 vs 17.35 calculated on account of interference from antimony.

(ii) Synthesis of $[\text{Hg}_2(\text{CO})_2][\text{Sb}_2\text{F}_{11}]_2$. To 722 mg (1.64 mmol) of Hg_2F_2 contained in part A of the reactor (see Figure 1) was added *in vacuo* about 2 mL of HSO_3F . On heating the reactor to $80\text{ }^\circ\text{C}$, effervescence was noted and the color of the yellow suspension turned to light yellow. After removal of all volatile materials (HF , SiF_4 , HSO_3F), about 1 mL of SbF_5 was added. Continuous stirring and heating of the mixture to $90\text{ }^\circ\text{C}$ and a CO pressure of 500 mbar produced a homogeneous light yellow solution. When the reaction mixture was concentrated *in vacuo*, a very viscous residue remained. To this residue were added another 5 mL of SbF_5 and about 700 mbar CO. At $100\text{ }^\circ\text{C}$, a small amount of a white precipitate had formed suspended in SbF_5 . The temperature was lowered to $60\text{ }^\circ\text{C}$ and the CO pressure raised to 1 atm. Rapid CO uptake occurred and resulted in the formation of more precipitate. After 1 h the CO uptake had stopped. Separation of the cream colored solid from the excess of SbF_5 was carried out as described above for $[\text{Hg}(\text{CO})_2][\text{Sb}_2\text{F}_{11}]_2$. Since slow release of CO at room temperature was noted, the product was only dried briefly *in vacuo*. A total mass of 2115 mg (1.55 mmol) was obtained, which suggested a yield of 94%.

The solid started shrinking at $100\text{ }^\circ\text{C}$ and melted at $140\text{ }^\circ\text{C}$ when heated in a sealed tube. The equilibrium CO pressure at 20 and $60\text{ }^\circ\text{C}$ was 8 and 60 mbar, respectively. In an evacuated flask, all CO was given off within 30 min at a temperature of $50\text{ }^\circ\text{C}$.

(iii) Synthesis of $[\text{Hg}(^{13}\text{C}\text{O})_2][\text{Sb}_2\text{F}_{11}]_2$ and $[\text{Hg}_2(^{13}\text{C}\text{O})_2][\text{Sb}_2\text{F}_{11}]_2$. The syntheses were accomplished as described in (i) and (ii). Unreacted

(30) Willner, H.; Bodenbinder, M.; Wang, C.; Aubke, F. *J. Chem. Soc., Chem. Commun.* **1994**, 1189.

(31) Barr, J.; Gillespie, R. J.; Thompson, R. C. *Inorg. Chem.* **1964**, 3, 1149.

(32) (a) Cady, G. H.; Shreeve, J. M. *Inorg. Synth.* **1963**, 7, 124. (b) Cady, G. H. *Inorg. Synth.* **1968**, 11, 155.

(33) Mallela, S. P.; Aubke, F. *Can. J. Chem.* **1984**, 62, 382.

Table 1. Crystallographic Data for the Structure Determination of $[\text{Hg}(\text{CO})_2][\text{Sb}_2\text{F}_{11}]_2$ at 195 K

chem formula	$\text{HgSb}_4\text{F}_{22}\text{O}_2\text{C}_2$	cryst syst	monoclinic
fw	1161.56	space group	$P2_1/n$
a (Å) ^a	7.607(2)	ρ_c (g cm ⁻³)	3.989
b (Å)	14.001(3)	λ (Mo $K\alpha_1$) (Å)	0.70930
c (Å)	9.730(2)	μ (Mo $K\alpha$) (cm ⁻¹)	136.7
β (deg)	111.05(2)	min-max 2θ (deg)	4-57
V (Å ³)	967.1	transmission ^b	0.032-0.108
Z	2	cryst dimensions	0.23 × 0.33 × 0.40
R_f^c	0.035	R_{wF}^d	0.046

^a Cell dimensions were determined from 25 reflections ($40^\circ \leq 2\theta \leq 52^\circ$). ^b The data were corrected for the effects of absorption, by the Gaussian integration method. ^c $R_f = \sum(|F_o| - |F_c|)/\sum|F_o|$, for 1983 data ($I_o \geq 2.5\sigma(I_o)$). ^d $R_{wF} = [\sum(w(|F_o| - |F_c|)^2)/\sum(wF_o^2)]^{1/2}$ for 1983 data ($I_o \geq 2.5\sigma(I_o)$); $w = [\sigma(F_o)^2 + 0.0005F_o^2]^{-1}$.

¹³C O was absorbed on molecular sieves (Merck, 5 Å) at -196°C and recovered for reuse at elevated temperatures.

(d) Crystal Growth. To a 0.5 M solution of $\text{Hg}(\text{SO}_3\text{F})_2$ in $\text{HSO}_3\text{F}-\text{SbF}_5$ (mole ratio $\text{HSO}_3\text{F}:\text{SbF}_5 \sim 1:2$) contained in the reactor shown in Figure 1 was admitted CO gas, with the reactor kept at 70°C . On CO addition immediate precipitation occurred. The precipitate was redissolved and the CO pressure adjusted to ~ 600 mbar at 70°C . The solution was allowed to cool to room temperature at a rate of $10^\circ\text{C}/\text{day}$. The crystal needles produced had edge lengths of up to 1 mm. The supernatant solution was decanted, and the crystals were washed with $\text{C}_4\text{F}_9\text{SO}_2\text{F}$ and dried *in vacuo* with the reactor at room temperature.

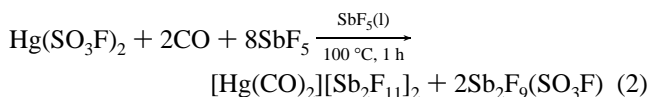
(e) X-ray Crystallography. Under dry nitrogen atmosphere, a fragment was cleaved from a colorless crystal and was gently wedged in a capillary tube with a trace of fluorocarbon grease as an adhesive. The tube was hot-wire sealed in the glovebox. Data were recorded at 195 K with an Enraf Nonius CAD4F diffractometer equipped with an in-house modified low-temperature attachment. Graphite monochromatized Mo $K\alpha$ radiation was used. Intensity standards (2 every hour) showed no decay until near the end of data acquisition, when there was a single $\sim 5\%$ drop in intensity resulting from a momentary interruption of the low-temperature control. The data were corrected for the effects of absorption by the Gaussian integration method, and corrections were carefully checked against measured ψ scans. Data reduction included corrections for intensity scale variation and for Lorentz and polarization effects.

The structure was solved by direct methods. The final full-matrix least squares refinement of 143 parameters, using 1983 data ($I_o \geq 2.5\sigma(I_o)$), included appropriate coordinates and anisotropic thermal parameters for all atoms and an extinction parameter.³⁴ A weighting scheme based on counting statistics was applied such that $\langle w(|F_o| - |F_c|)^2 \rangle$ was near constant at a function of both $|F_o|$ and $(\sin \theta)/\lambda$. The refinement converged at $R_f = 0.035$ and $R_{wF} = 0.046$.

The programs used for the structure determination were from the NRCVAX Crystal Structure System³⁵ and CRYSTALS.³⁶ Complex scattering factors for neutral atoms³⁷ were used in the calculation of structure factors. Computations were carried out on MicroVAX-II and 80486 computers. Crystallographic details are summarized in Table 1. Final fractional atomic coordinates are listed in Table 2.

Results and Discussion

(a) Synthetic Aspects. The synthesis of $[\text{Hg}(\text{CO})_2][\text{Sb}_2\text{F}_{11}]_2$ is accomplished in a straightforward manner according to:

**Table 2.** Atomic Coordinates^a and Equivalent Isotropic Thermal Parameters (Å²) for $[\text{Hg}(\text{CO})_2][\text{Sb}_2\text{F}_{11}]_2$ at 195 K

atom	x	y	z	U_{eq}^b
Hg	0.500	0.000	0.000	0.0303
Sb(1)	1.03217(7)	-0.08300(3)	0.24945(6)	0.0255
Sb(2)	0.67314(6)	-0.22666(3)	0.36746(5)	0.0232
F(1)	0.9054(7)	-0.1548(3)	0.3667(5)	0.033
F(12)	0.8053(6)	-0.1020(4)	0.0860(6)	0.037
F(13)	0.9079(10)	0.0230(4)	0.2812(9)	0.054
F(14)	1.2304(8)	-0.0662(4)	0.4239(7)	0.049
F(15)	1.1151(8)	-0.2009(4)	0.2175(7)	0.045
F(16)	1.1486(8)	-0.0198(4)	0.1390(7)	0.045
F(22)	0.8428(7)	-0.3252(3)	0.4632(5)	0.033
F(23)	0.7246(8)	-0.1651(3)	0.5440(5)	0.038
F(24)	0.5424(7)	-0.1201(3)	0.2656(6)	0.036
F(25)	0.6700(7)	-0.2766(3)	0.1909(5)	0.035
F(26)	0.4648(7)	-0.2926(4)	0.3718(6)	0.041
O	0.4959(10)	0.0986(5)	0.2940(8)	0.045
C	0.4943(11)	0.0632(6)	0.1921(11)	0.033

^a The general equivalent positions in the space group $P2_1/n$ are: $x, y, z; -x, -y, -z; 1/2 - x, 1/2 + y, 1/2 - z; 1/2 + x, 1/2 - y, 1/2 + z$. ^b The equivalent isotropic thermal parameter is the cube root of the product of the principal axes of the thermal ellipsoid.

Repeated washing with perfluorobutyl sulfonyl fluoride, $\text{C}_4\text{F}_9\text{SO}_2\text{F}$, provides a convenient way to separate the solid product from the excess of antimony(V) fluoride. Subsequent studies have shown that, for $[\text{Hg}(\text{CO})_2][\text{Sb}_2\text{F}_{11}]_2$, the choice of solvents or inert liquid media is very limited. For example, SO_2 and HSO_3F , both suitable for $[\text{Au}(\text{CO})_2][\text{Sb}_2\text{F}_{11}]_4$ cause evolution of CO. It appears that $[\text{Hg}(\text{CO})_2]^{2+}$ is a stronger electrophile than isoelectronic $[\text{Au}(\text{CO})_2]^+$. Hence, fluorosulfuric acid, HSO_3F , which has been a satisfactory medium for the generation in solution of all so far known nonclassical carbonyl cations,^{3a,9} is unsatisfactory. Its self-ionization ion, SO_3F^- , is sufficiently basic and will partly displace CO to produce eventually the starting material $\text{Hg}(\text{SO}_3\text{F})_2$. Addition of 2 mol of SbF_5/mol of HSO_3F will reduce the anion basicity sufficiently to allow the growth of crystals of $[\text{Hg}(\text{CO})_2][\text{Sb}_2\text{F}_{11}]_2$ and to obtain ¹³C NMR spectra. The formation reaction seems to proceed quantitatively. The facile synthesis, the near quantitative yield, and the relatively high thermal stability of $[\text{Hg}(\text{CO})_2][\text{Sb}_2\text{F}_{11}]_2$ are surprising. It appears that neither thermodynamic instability nor kinetic reasons, e.g., favorably competing reactions, are responsible for the lack of previous reports on carbonyls of mercury or of any other post-transition metal. Reliance on the noble gas formalism and the synergetic bonding model, with π -back-donation an essential feature, may have contributed to a reluctance to extend the search for metal carbonyls beyond the transition metals in low oxidation states. In addition, the existence of isoelectronic cyanide derivatives of electron rich metals^{23,24} like Pd, Pt, Au, Ag, and Hg, with π -back-bonding non-essential here, has not resulted prior to our work^{3a,4} in the inference that these metals should also form stable, isoelectronic carbonyl cations.

There has also been a lack of suitable and convenient synthetic routes to the carbonyl cations. The role of strong protonic acids like HSO_3F , used in the synthesis of $\text{Hg}(\text{SO}_3\text{F})_2$ ³³ or of magic acid ($\text{HSO}_3\text{F}-\text{SbF}_5$), employed to recrystallize $[\text{Hg}(\text{CO})_2][\text{Sb}_2\text{F}_{11}]_2$, has been largely limited to the generation of CO containing transition metal cations by protonation of metal carbonyl derivatives¹⁵ and, starting with the pioneering study

(34) Larson, A. C. In *Crystallographic Computing*; Ahmed, F. R., Ed.; Munksgaard: Copenhagen, 1970; p 293.

(35) Gabe, E. J.; LePage, Y.; Charland, J.-P.; Lee, F. L.; White, P. S. NRCVAX—An Interactive Program System for Structure Analysis. *J. Appl. Cryst.* **1989**, *22*, 384.

(36) Watkin, D. J.; Carruthers, J. R.; Betteridge, P. W. CRYSTALS, Chemical Crystallography Laboratory, University of Oxford, Oxford, England, 1984.

(37) *International Tables for X-ray Crystallography*; Kynoch Press: Birmingham, England, 1975; Vol. IV, p 99.

by Manchot and König,³⁸ to the generation of solvated copper(I) and silver(I) carbonyl cations³⁹ as reactive intermediates in solution and their use in carbonylation reactions.⁴⁰ In addition, the cleavage of metal–CO bonds by protolysis has found wide use in synthesis, as exemplified by the classical preparation of Mo(II) carboxylates from Mo(CO)₆.⁴¹

The solvolytic conversion of element fluorosulfates to fluoroantimonates in liquid antimony(V) fluoride has been used by us in the past^{42–44} to generate main group (I₂⁺),⁴² organometallic ((CH₃)₂Sn²⁺),⁴³ or metallic (Pd²⁺)⁴⁴ cations stabilized by the very weakly basic anions like [SbF₆][−] or [Sb₂F₁₁][−].^{42,43} The adaptation of this approach to the generation of salts containing the carbonyl cations [Pd(CO)₄]²⁺, [Pt(CO)₄]²⁺,⁵ or [Au(CO)₂]⁺⁴ is very recent and involves reagent combinations, which are unusual and not widely available in organometallic laboratories.

While the field of nonclassical metal carbonyl cations is still small, and hopefully expandable, it is noted that all thermally stable salts reported so far involve the undecafluorodiantimonate(V) anion [Sb₂F₁₁][−]. In [Pt(CO)₄][Pt(SO₃F)₆],⁷ the sole exception, the [Pt(SO₃F)₆]^{2−} anion, is a comparably weak nucleophile to [SbF₆][−] or [Sb₂F₁₁][−].¹³ The anion [Sb₂F₁₁][−] appears to be particularly well suited to the stabilization of highly electrophilic, nonclassical carbonyl cations.

While CO addition to various Ag⁺ salts of complex teflates like [B(OTeF₅)₄] has been successful and has allowed the determination of two interesting structures,^{1,2,45} it is anticipated that CO addition will be more difficult and CO elimination more facile for salts with M²⁺ or M³⁺ cations on account of the considerably larger lattice energies of the precursor salts. The difference in lattice energies of [M(CO)_n]ⁿ⁺ salts versus Mⁿ⁺ species will be reduced somewhat, where very large, weakly coordinating anions are employed.^{1,2,45,46}

The relatively high thermal stability of [Hg(CO)₂][Sb₂F₁₁]₂ is surprising. Decomposition reactions to produce Hg[Sb₂F₁₁]₂, Hg[SbF₆]₂, or HgF₂ should be facile and thermodynamically feasible on account of the higher lattice energies expected for the mercury(II) fluoroantimonates or for HgF₂, unless there is additional stabilization of the [Hg(CO)₂]²⁺ cation by the [Sb₂F₁₁][−] anions in the solid state, resulting in a marked increase of the lattice energy of [Hg(CO)₂][Sb₂F₁₁]₂.

The synthesis of [Hg₂(CO)₂][Sb₂F₁₁]₂ proceeds in a similar manner and with comparable ease to the preparation of [Hg(CO)₂][Sb₂F₁₁]₂ as discussed above. There are two additional problems with the synthesis and characterization of this material. First, the thermal stability of the resulting product is low, and a measurable dissociation pressure of CO at 25 °C restricts identification to the mass balance of the reaction and vibrational as well as ¹³C NMR spectra. Second, while the original synthesis, as reported previously³⁰ and described in the Experimental Section, produces [Hg₂(CO)₂][Sb₂F₁₁]₂ in a straightforward manner with the product used in the spectroscopic characterization, in subsequent preparations variable small amounts of [Hg(CO)₂][Sb₂F₁₁]₂ are detected by the unusually

Table 3. Vibrational Data for [Hg(CO)₂][Sb₂F₁₁]₂, [Hg₂(CO)₂][Sb₂F₁₁]₂, and Hg₂[Sb₂F₁₁]₂

[Hg(CO) ₂][Sb ₂ F ₁₁] ₂		[Hg ₂ (CO) ₂][Sb ₂ F ₁₁] ₂		Hg ₂ [Sb ₂ F ₁₁] ₂	assignment
IR	Raman	IR	Raman	Raman	
	2281 s		2248 m		ν _s (CO)
	2228 vw		2197		ν _s (¹³ CO)
2278 m		2247 m			ν _{as} (CO)
2225 vw		2196 vw			ν _{as} (¹³ CO)
729 s					
	723 m		722 w		
716 s					
698 s	698 s	693 s			
	670 sh	679 vs	678 m	672 sh	
666 vs	663 vs		667 m, sh		
	653 sh	657 s	657 vs	659 vs	Sb ₂ F ₁₁
640 vs		643 s	642 sh		
584 s	588 m		597 s		
575 s	575 m			560 vw	
491 s		493 m			
335 m					ν _{as} (HgC)/ δ(CHgC)
325 m					ν _{as} /δ ¹³ C
311 m					
	302 m		298 w	292 m	
	287 m		282 m		
275 sh			273 w		Sb ₂ F ₁₁
260 s					
	231 m				
227 vs			225 w		
	215 w				
			169 s	190 s	ν(Hg–Hg)
			167 m		ν(Hg–Hg)(¹³ C)

high CO stretching vibration (vide infra) and by its ¹³C NMR spectrum. It appears that partial oxidation to Hg(II) has occurred during the synthesis. Both SbF₅ and SO₃, formed by elimination from an Sb–SO₃F group at ~60 °C, are potential oxidizing agents. We have so far been unable either to find conditions where this side reaction is suppressed or to reproduce the original preparation. Alternatively, disproportionation⁴⁷ of Hg₂²⁺ to Hg²⁺ and Hg⁰ may be considered, but this reaction occurs in a basic medium, and Hg should be detectable by its black color. Disproportionation has, e.g., prevented the synthesis of Hg₂(CN)₂, isoelectronic to the cation [Hg₂(CO)₂]²⁺, which is only detected as a short-lived intermediate in the pulse radiolysis of Hg(CN)₂ in H₂O.⁴⁸

A precedent for [Hg₂(CO)₂]²⁺ may be found in cations of the type [Hg₂(PF₃)_n]²⁺,⁴⁸ n = 1 or 2, formed by the addition of PF₃ to Hg₂[AsF₆]₂ in SO₂ and detected by ¹⁹F and ³¹P NMR and Raman spectroscopy at 0 °C.⁴⁹ The cations appear to decompose quickly at room temperature to PF₅ and AsF₃. For these and other PR₃ complexes of mercury(I), evidence from ¹⁹F and ³¹P NMR is cited that suggests little or no π-back-donation from Hg to PF₃.

Thermal decomposition of [Hg₂(CO)₂][Sb₂F₁₁]₂ at 50 °C *in vacuo* results in the quantitative formation of Hg₂[Sb₂F₁₁]₂, which does not seem to have been described previously. The reaction of mercury with SbF₅ in liquid SO₂ is reported to produce Hg₃[Sb₂F₁₁]₂^{50,51} instead. A characterization of Hg₂[Sb₂F₁₁]₂ is restricted to its Raman spectrum discussed below.

(b) Vibrational Spectra. The observed band positions for [Hg(CO)₂][Sb₂F₁₁]₂ and [Hg₂(CO)₂][Sb₂F₁₁]₂ obtained from Raman and IR spectra are listed in Table 3 together with selected

(38) Manchot, W.; König, J. *Chem. Ber.* **1927**, *60*, 2183.

(39) Souma, Y.; Iyoda, J.; Sano, H. *Inorg. Chem.* **1976**, *15*, 968.

(40) (a) Souma, Y.; Sano, H. *J. Org. Chem.* **1973**, *38*, 2016. (b) Souma, Y.; Sano, H. *Bull. Chem. Soc. Jpn.* **1973**, *46*, 3273. (c) Souma, Y.; Sano, H. *J. Org. Chem.* **1973**, *38*, 3633.

(41) Stephenson, T. A.; Bannister, E.; Wilkinson, G. *J. Chem. Soc.* **1964**, 2538.

(42) Wilson, W. W.; Thompson, R. C.; Aubke, F. *Inorg. Chem.* **1980**, *19*, 1489.

(43) Mallela, S. P.; Yap, S.; Sams, J. R.; Aubke, F. *Rev. Chim. Miner.* **1986**, *23*, 572.

(44) Cader, M. S. R.; Aubke, F. *Can. J. Chem.* **1989**, *67*, 1700.

(45) Hurlburt, P. K.; Rack, J. J.; Luck, J. S.; Dec, S. F.; Webb, J. D.; Andersen, O. P.; Strauss, S. H. *J. Am. Chem. Soc.* **1994**, *116*, 10003.

(46) Strauss, S. H. *Chem. Rev.* **1993**, *93*.

(47) Roberts, H. L. *Adv. Inorg. Chem. Radiochem.* **1968**, *11*, 309.

(48) Fujita, S.; Horii, H.; Mori, T.; Taniguchi, S. *Bull. Chem. Soc. Jpn.* **1975**, *48*, 3067.

(49) Dean, P. A. W.; Ibbott, D. G. *Can. J. Chem.* **1976**, *54*, 177.

(50) Cutforth, B. D.; Davies, C. G.; Dean, P. A. W.; Gillespie, R. J.; Ireland, P. R.; Ummat, P. K. *Inorg. Chem.* **1973**, *12*, 1343.

(51) Gillespie, R. J.; Passmore, J. *Adv. Inorg. Chem. Radiochem.* **1975**, *17*, 79.

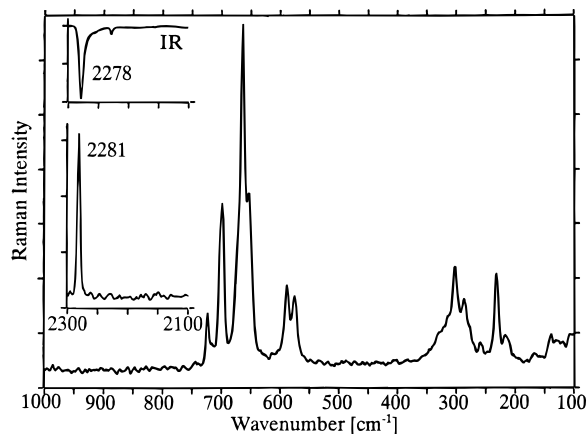


Figure 2. Raman spectrum of $[\text{Hg}(\text{CO})_2][\text{Sb}_2\text{F}_{11}]_2$.

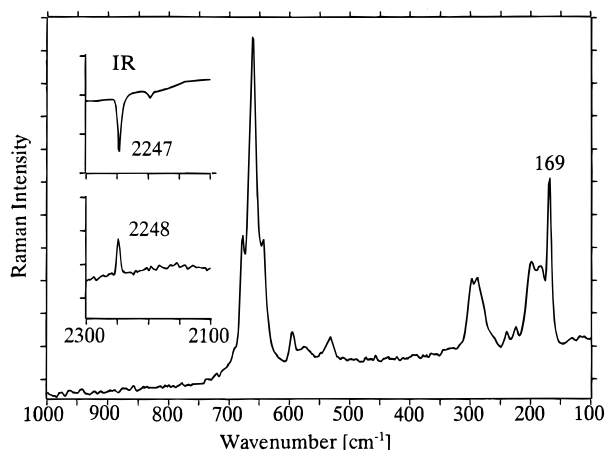


Figure 3. Raman spectrum of $[\text{Hg}_2(\text{CO})_2][\text{Sb}_2\text{F}_{11}]_2$.

band positions for the ^{13}C isotopomers. Also listed are Raman shifts for $\text{Hg}_2[\text{Sb}_2\text{F}_{11}]_2$. The Raman spectrum of $[\text{Hg}(\text{CO})_2][\text{Sb}_2\text{F}_{11}]_2$ is shown in Figure 2, while Figure 3 shows the Raman spectra of $[\text{Hg}_2(\text{CO})_2][\text{Sb}_2\text{F}_{11}]_2$.

Vibrational identification of the two cations $[\text{Hg}(\text{CO})_2]^{2+}$ and $[\text{Hg}_2(\text{CO})_2]^{2+}$ is limited to the CO stretching regions for two reasons. (i) As noted previously for $[\text{Au}(\text{CO})_2]^{+4}$ and $\text{Hg}(\text{CN})_2$,²⁷ the remaining fundamentals are usually of very low intensity and are observed below 500 cm^{-1} , where intense anion bands are found.^{4,5} (ii) In contrast to observations made for $[\text{Au}(\text{CO})_2][\text{Sb}_2\text{F}_{11}]$,⁴ bands due to the anion $[\text{Sb}_2\text{F}_{11}]^-$ are more complex for the two carbonyl derivatives described here. Bands are extensively split, and some do coincide in the Raman and IR spectra. It can be concluded that the symmetry of the anion must be lower than D_{4h} . The extensive band splitting makes it more difficult to recognize other cation bands, even though the complete vibrational spectra of $[\text{Hg}(^{13}\text{C})_2][\text{Sb}_2\text{F}_{11}]_2$ and $[\text{Hg}_2(^{13}\text{C})_2][\text{Sb}_2\text{F}_{11}]_2$ have been obtained in this study.

A much simpler vibrational spectrum is obtained for $\text{Hg}_2[\text{Sb}_2\text{F}_{11}]_2$, which suggests possibly a return to D_{4h} symmetry for the anion. A rather similar Raman spectrum is reported for $\text{Hg}_3[\text{Sb}_2\text{F}_{11}]_2$ ⁵⁰ in the anion region, where bands at 683 (w), 644 (vs), 630 (w), 544 (w), and 291 (s) have previously been observed.⁵⁰

For $\text{Hg}_2[\text{Sb}_2\text{F}_{11}]_2$, $\bar{\nu}(\text{Hg}-\text{Hg})$ is found unprecedentedly high at 190 cm^{-1} . For $\text{Hg}_2[\text{AsF}_6]_2$, this band is observed at 180 cm^{-1} ,^{50,51} and for solutions containing Hg_2^{2+} , a value of 182 cm^{-1} is reported.⁵² This observation confirms our contention

that $[\text{Sb}_2\text{F}_{11}]^-$ ranks among the weakest nucleophiles, in agreement with observations made for a series of Xe(II) fluoro cations.⁵³ A direct relationship between $\bar{\nu}(\text{Hg}-\text{Hg})$, the Hg-Hg bond distance, and the electronegativity of the ligand X for mercurous compounds of the type Hg_2X_2 has previously been reported,⁵⁴ and it can be concluded that for $\text{Hg}_2[\text{Sb}_2\text{F}_{11}]_2$ the Hg-Hg distance should be comparable or slightly shorter than for Hg_2F_2 , where $\bar{\nu}(\text{Hg}-\text{Hg})$ is 185.9 cm^{-1} and the Hg-Hg bond distance is $2.43(3)$.⁵⁵

Addition of 2 mol of CO to Hg_2^{2+} to give $[\text{Hg}_2(\text{CO})_2]^{2+}$ results in a shift of $\bar{\nu}(\text{Hg}-\text{Hg})$ to lower wavenumbers. For the cation with CO at the natural isotope distribution, $\bar{\nu}(\text{Hg}-\text{Hg})$ is at 169 cm^{-1} , while for $[\text{Hg}_2(^{13}\text{C})_2]^{2+}$ $\bar{\nu}(\text{Hg}-\text{Hg})$ is found 2 wavenumbers lower, which suggests vibrational mixing of Hg-Hg with Hg-C stretching vibrations.

In the CO stretching range, a number of unusual features are noted for both $[\text{Hg}(\text{CO})_2]^{2+}$ and $[\text{Hg}_2(\text{CO})_2]^{2+}$. The band positions are shifted to high wavenumbers, and the values of 2281 and 2278 cm^{-1} (ν_1 and ν_3 , respectively, with $\bar{\nu}_{\text{av}}$ at 2279.5 cm^{-1}) observed for $[\text{Hg}(\text{CO})_2]^{2+}$ are so far the highest $\bar{\nu}(\text{CO})$ values for any metal carbonyl, well above $\bar{\nu}_{\text{av}}(\text{CO})$ of 2261 and 2235 cm^{-1} for $[\text{Pt}(\text{CO})_4]^{2+5}$ and for $[\text{Au}(\text{CO})_2]^{+4}$, respectively. The stretching force constant f_s , calculated using a two mass model, is $(21.0 \pm 0.1) \times 10^2\text{ N m}^{-1}$, very close to $21.3 \times 10^2\text{ N m}^{-1}$ obtained for HCO^+ ,⁴ and the claim that π -back-bonding is absent is in this case justified.

Equally unusual for metal carbonyl cations is the very small separation between the Raman-active ν_1 mode at 2281 and the IR-active ν_3 mode at 2278 cm^{-1} , which signifies strongly diminished coupling due to very weak Hg-C bonds, consistent with the absence of π -back-bonding. Similarly small separations between $\bar{\nu}(\text{CN})$ fundamentals are found for solid $\text{Hg}(\text{CN})_2$ ²⁷ and for $[\text{Ag}(\text{CN})_2]^-$.^{25,56} In all instances substantially reduced metal to carbon π -back-bonding results in very weak metal-carbon and strong intraligand (C-N or C-O) bonds.

For the mercury(I) carbonyl cation $[\text{Hg}_2(\text{CO})_2]^{2+}$, slightly lower values for the symmetric and asymmetric $\bar{\nu}(\text{CO})$ stretches (2248 and 2247 cm^{-1}) and f_s ($20.4 \times 10^2\text{ N m}^{-1}$) are observed or calculated, compared to the corresponding data for $[\text{Hg}(\text{CO})_2]^{2+}$. Again, the separation between both bands is very small, and evidence for linearity of the $[\text{Hg}_2(\text{CO})_2]^{2+}$ cation rests with the observation that $\bar{\nu}(\text{Hg}-\text{Hg})$ is only Raman-active. Our contention, based on isotope $^{12}\text{C}/^{13}\text{C}$ shifts, that the band observed at 169 may not be a pure Hg-Hg vibration, is supported by a report on Raman spectra of $\text{Hg}_2[\text{AsF}_6]_2$ complexes with heavier group 15 and 16 donor ligands.⁴⁹ Here, $\nu(\text{Hg}-\text{Hg})$ decreases with increasing mass of the donor atom from 173 to 110 cm^{-1} , consistent with vibrational coupling.

To summarize the discussion on the vibrational spectra of the new mercury carbonyl cations in the CO stretching range, the relevant data are collected in Table 4 together with the corresponding data for those linear carbonyl and cyanide species, where assignments are in all instances supported and confirmed by vibrational studies of the ^{13}C isotopomers and where force constants are known. To limit counterion effects, only K^+ and $[\text{Sb}_2\text{F}_{11}]^-$ salts are included in the tabulation. Also included are data for $[\text{HCO}]^+$ ^{4,57} and HCN ^{25,58} which within each group exhibit the highest C-X ($\text{X} = \text{O}$ or N) stretching force constants f_s . In both molecules π -back-bonding is impossible. It is noted

(53) Gillespie, R. J.; Landa, B. *Inorg. Chem.* **1973**, *12*, 1383.

(54) Stammreich, H.; Teixeira Sans, T. *J. Mol. Struct.* **1967-68**, *1*, 55.

(55) Grdenic, D.; Djordjevic, C. *J. Chem. Soc.* **1956**, 1316.

(56) Jones, L. H. *J. Chem. Phys.* **1957**, *26*, 1578.

(57) Foster, S. C.; McKellar, A. R. W.; Sears, T. J. *J. Chem. Phys.* **1984**, *81*, 578.

(58) Suzuki, I.; Pariseau, M. A.; Overend, J. J. *J. Chem. Phys.* **1966**, *44*, 3561.

(52) Davies, C. G.; Dean, P. A. W.; Gillespie, R. J.; Ummat, P. K. *J. Chem. Soc., Chem. Commun.* **1971**, 782.

Table 4. CO and CN Stretching Vibration and Stretching Force Constants for Linear Dicarbonyl and Dicyanide Species with ^{13}C Data in Brackets

compd	$\nu_1(\text{CX})$ (cm^{-1})	$\nu_3(\text{CX})$ (cm^{-1})	$f_r \times 10^2$ (N m^{-1})	ref
$[\text{Hg}(\text{CO})_2][\text{Sb}_2\text{F}_{11}]_2$	2281 (2228)	2278 (2225)	21.0 ± 0.1	this work
$\text{Hg}(\text{CN})_2$	2197.4 (2148)	2197.2 (2149)	18.07 ± 0.15	25, 60
$[\text{Au}(\text{CO})_2][\text{Sb}_2\text{F}_{11}]$	2254 (2194.5)	2217 (2160)	20.1 ± 0.1	4
$\text{K}[\text{Au}(\text{CN})_2]$	2164 (2115.6)	2146 (2099)	17.64 ± 0.1	25, 60, 61
$\text{K}[\text{Ag}(\text{CN})_2]$	2146	2140 (2093.5)	17.04 ± 0.2	25, 56, 61
$[\text{HCO}]^+(\text{g})^a$	2184		21.3 ± 0.1	4, 57
HCN	2096.7		18.8 ± 0.1	25, 58
$[\text{Hg}_2(\text{CO})_2][\text{Sb}_2\text{F}_{11}]_2$	2248 (2197)	2247 (2196)	20.4 ± 0.1	this work

^a Band is labeled ν_3 in ref 57.

Table 5. Selected Distances (\AA) and Angles (deg) for $\text{Hg}(\text{CO})_2[\text{Sb}_2\text{F}_{11}]_2$

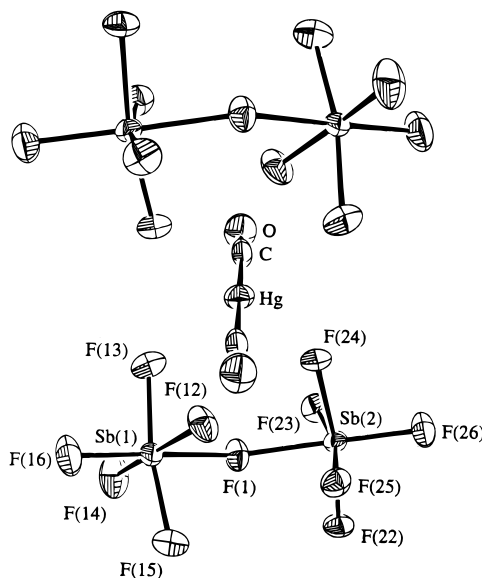
Hg—C	2.083(10)	Hg—F(12)	2.595(5)	
O—C	1.104(12)	Hg—F(22) ^b	2.691(4)	
Sb(1)—F(1)	2.008(4)	Sb(2)—F(1)	2.035(4)	2.042 ^a
Sb(1)—F(12)	1.899(5)	Sb(2)—F(22)	1.890(4)	1.899 ^a
Sb(1)—F(13)	1.844(6)	Sb(2)—F(23)	1.834(5)	1.846 ^a
Sb(1)—F(14)	1.836(6)	Sb(2)—F(24)	1.869(4)	1.880 ^a
Sb(1)—F(15)	1.833(5)	Sb(2)—F(25)	1.847(5)	1.857 ^a
Sb(1)—F(16)	1.845(5)	Sb(2)—F(26)	1.847(5)	1.864 ^a
C—F(12) ^c	2.895(10)	C—F(13)	3.002(10)	
C—F(16) ^d	2.749(9)	C—F(22) ^b	2.758(9)	
C—F(24)	2.653(9)	O—F(14) ^e	2.823(10)	
O—F(15) ^b	2.922(9)	O—F(23) ^f	2.840(8)	

Hg—C—O	177.7(7)	F(22) ^b —Hg—C	69.24(23)
F(12)—Hg—F(22) ^b	98.88(16)	Hg—F(12)—Sb(1)	129.2(3)
F(12)—Hg—C	104.4(3)	Hg—F(22) ^b —Sb(2) ^b	157.16(25)
F(1)—Sb(1)—F(12)	85.88(21)	F(1)—Sb(2)—F(22)	85.54(20)
F(1)—Sb(1)—F(13)	85.9(3)	F(1)—Sb(2)—F(23)	82.99(21)
F(1)—Sb(1)—F(14)	86.65(23)	F(1)—Sb(2)—F(24)	84.30(20)
F(1)—Sb(1)—F(15)	84.83(23)	F(1)—Sb(2)—F(25)	84.53(21)
F(1)—Sb(1)—F(16)	178.5(3)	F(1)—Sb(2)—F(26)	178.92(22)
F(12)—Sb(1)—F(13)	83.5(3)	F(22)—Sb(2)—F(23)	90.18(22)
F(12)—Sb(1)—F(14)	171.7(3)	F(22)—Sb(2)—F(24)	169.58(21)
F(12)—Sb(1)—F(15)	89.8(3)	F(22)—Sb(2)—F(25)	87.74(21)
F(12)—Sb(1)—F(16)	93.53(24)	F(22)—Sb(2)—F(26)	93.65(23)
F(13)—Sb(1)—F(14)	92.4(3)	F(23)—Sb(2)—F(24)	90.89(23)
F(13)—Sb(1)—F(15)	168.9(3)	F(23)—Sb(2)—F(25)	167.47(23)
F(13)—Sb(1)—F(16)	95.4(3)	F(23)—Sb(2)—F(26)	96.30(24)
F(14)—Sb(1)—F(15)	93.1(3)	F(24)—Sb(2)—F(25)	88.97(22)
F(14)—Sb(1)—F(16)	94.0(3)	F(24)—Sb(2)—F(26)	96.53(23)
F(15)—Sb(1)—F(16)	93.8(3)	F(25)—Sb(2)—F(26)	96.16(24)
Sb(1)—F(1)—Sb(2)	147.6(3)		

^a Distances corrected for thermal motion using a riding model. ^b $3/2 - x, 1/2 + y, 1/2 - z$. ^c $1 - x, -y, -z$. ^d $-1 + x, y, z$. ^e $2 - x, -y, 1 - z$. ^f $1 - x, -y, 1 - z$.

that for both HCN and HCO^+ , the C—X (X = N or O) stretching vibrations are observed at relatively low wavenumbers of 2096.7 and 2184 cm^{-1} , respectively.²⁵ This is obviously due to vibrational mixing with ν_3 , the CH vibration, evident from the H/D isotope shift for $\bar{\nu}(\text{CN})$ in HCN^{25,58} from 2096.7 to 1925.3 cm^{-1} . A similar situation pertains to HCO^+ . A more detailed tabulation of vibrational data for all known nonclassical carbonyl cations has appeared elsewhere.⁵⁹ Data for the $[\text{M}(\text{CN})_2]^-$, M = Ag or Au, are those of the solid potassium salts.^{56,60}

In both the carbonyl and the cyanide series, the mercury(II) species exhibit the highest $\bar{\nu}(\text{CX})$, values (X = O or N) and the highest force constants, exceeded only by those for HCO^+ ⁴ and HCN,^{25,58} and the smallest band separation between ν_1 and ν_3 . Only for $[\text{Hg}_2(\text{CO})_2]^{2+}$ is a similar small band separation observed. Hence, $[\text{Hg}(\text{CO})_2]^{2+}$ and the isoelectronic cyanide $\text{Hg}(\text{CN})_2$ are the closest approaches to “ σ -only bonding” for both groups of metal complexes. For the two isoelectronic gold(I) species, $[\text{Au}(\text{CO})_2]^+$ ⁴ and $[\text{Au}(\text{CN})_2]^-$,⁶⁰ the C—X (X = O

**Figure 4.** Molecular structure of $[\text{Hg}(\text{CO})_2][\text{Sb}_2\text{F}_{11}]_2$. 50% probability thermal ellipsoids are shown.

or N) stretching vibrations have shifted to lower values by 44 and 42 cm^{-1} , respectively, on account of the reduction in ionic complex charge. Wider separations between ν_1 and ν_3 are observed now, which suggests increased vibrational coupling and implies stronger M—C bonds in the gold(I) species. This is reflected also in an increase in f_R , the M—C force constant from $2.61 \times 10^2 \text{ N m}^{-1}$ for $\text{Hg}(\text{CN})_2$ to $2.81 \times 10^2 \text{ N m}^{-1}$ for $[\text{Au}(\text{CN})_2]^-$.^{25,61} For $[\text{Ag}(\text{CN})_2]^-$,⁵⁶ f_R decreases to $1.83 \times 10^2 \text{ N m}^{-1}$,⁶¹ and observed ν_1 — ν_3 separations for $[\text{Ag}(\text{CO})_2]^+$ and $[\text{Ag}(\text{CN})_2]^-$ are rather small.

(c) Molecular Structure of $[\text{Hg}(\text{CO})_2][\text{Sb}_2\text{F}_{11}]_2$. **(i) Description of the Structure.** The unique bond distances and angles are given in Table 5, as are the significant unique interionic distances. Corrections to bond lengths⁶² for thermal motion, using a model in which each fluorine atom is considered to be riding on the respective antimony atom and oxygen on carbon, are included in Table 5. The relatively small thermal motion of the carbon atom, probably on account of interionic C—F contacts (vide infra), supports such a model.

The $[\text{Hg}(\text{CO})_2]^{2+}$ cation which is nearly linear (Hg—C—O = 177.7(7)°) and has crystallographic inversion symmetry is shown in Figure 4 together with two neighboring, centrosymmetrically related $[\text{Sb}_2\text{F}_{11}]^-$ anions. The anion departs from D_{4h} symmetry and is distorted in several ways: (i) The Sb(1)—F(1)—Sb(2) bridge is bent (147.6(3)°) and slightly asymmetric. (ii) The two equatorial SbF_4 moieties of the dodecahedral anion are no longer eclipsed, and the four F atoms in each set are displaced toward the bridge. (iii) The F atoms within each

(59) Aubke, F. J. *Fluorine Chem.* **1995**, 72, 195.

(60) Jones, L. H. *J. Chem. Phys.* **1965**, 43, 594.

(61) Jones, L. H. *Inorg. Chem.* **1963**, 2, 777.

(62) Busing, W. R.; Levy, H. A. *Acta Crystallogr.* **1964**, 17, 142.

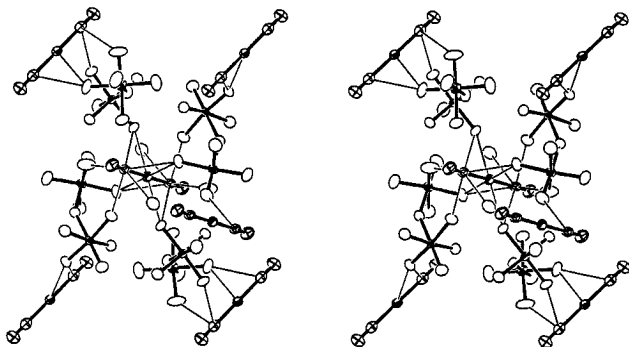


Figure 5. Stereo diagram depicting the significant interionic contacts in the crystal structure of $[\text{Hg}(\text{CO})_2][\text{Sb}_2\text{F}_{11}]_2$ (see text). 50% probability thermal ellipsoids are shown.

equatorial set are no longer strictly coplanar and equidistant to antimony. Sb–F terminal bond distances differ measurably (1.834(5)–1.899(5) Å), and bond angles are no longer uniform. The reason for these distortions is significant interionic contacts with $[\text{Hg}(\text{CO})_2]^{2+}$, which are now discussed in detail.

The mercury atom has four neighboring fluorine atoms at two unique distances: Hg–F(12) 2.595(5) Å and Hg–F(22)' 2.691(4) Å (where ' = $3/2 - x, 1/2 + y, 1/2 - z$), which are significantly shorter than the sum of the van der Waals radii for Hg and F (1.55 + 1.47 = 3.02 Å),⁶³ giving rise to a typical^{28b,64} distorted octahedral coordination environment about Hg. These weak Hg–F interactions produce an extended two-dimensional structure parallel to the major faces (1 0 –1) of the plate-shaped crystal. Within such a layer, each anion links a pair of cations and each cation links four anions.

There are, furthermore, five unique C–F close contacts (2.653(9)–3.002(10) Å), noticeably less than the sum of the respective van der Waals radii (3.17 Å).⁶³ Four of these supplement the two-dimensional extended structure already described. The fifth C–F contact (C–F(16)'' 2.749(9) Å (where '' = $-1 + x, y, z$)) links adjacent layers, thus producing a three-dimensional network in which the topology of anion–cation contacts is analogous to that in the rutile structure. Figure 5 is a stereoview of a portion of the extended two-dimensional structure which includes four complete anions and five cations. In addition, a fluorine atom and one $[\text{Hg}(\text{CO})_2]^{2+}$ cation from the layer above and a fluorine atom from the layer below are included to permit depiction of all Hg–F and C–F contacts for one cation (central) and one anion (lower left). Three terminal F–Sb bonds (F(12)–Sb(1) 1.899(5) Å; F(22)–Sb(2) 1.890(4) Å; F(24)–Sb(2) 1.869(5) Å) are significantly longer than the others (1.833(5)–1.847(5) Å), presumably as a (reasonable) consequence of the relative strengths of the corresponding F–Hg and F–C interactions.

Three unique O–F distances (2.823(10)–2.922(9) Å) and six unique F–F interionic distances (2.841(7)–2.901(7) Å) are also less than the appropriate sums of van der Waals radii for these elements (2.99 and 2.94 Å, respectively),⁶³ but they represent rather weaker (probably repulsive) interactions and are not shown in Figure 2. The fluorine atoms involved in the O–F contacts do not have close contacts to either mercury or carbon. There are no further interionic distances less than the appropriate sums of accepted van der Waals radii.⁶³

Interionic or intermolecular contacts involving Hg(II) are rather common.⁶⁴ Relevant examples are provided by HgCl_2 ^{65a} and $\text{Hg}(\text{CN})_2$,^{28b} where also distorted octahedral configurations

for the metal result with two sets of two Hg–Cl or Hg–N contacts. Secondary contacts involving the electrophilic C atom of the carbonyl group have recently been detected in *cis*-Pd(CO)₂(SO₃F)₂,⁹ where OC–OS intra- and intermolecular contacts range from 2.839(6) to 3.172(6) Å. The OC–FSb interionic contacts encountered for $[\text{Hg}(\text{CO})_2][\text{Sb}_2\text{F}_{11}]_2$ range from 2.653(9) to 3.002(10) Å. They appear to be stronger than in *cis*-Pd(CO)₂(SO₃F)₂, and the shorter distances are only partly explained by a slight decrease in van der Waals radii from O (1.52) to F (1.47).⁶³ It appears that both Hg–FSb and OC–FSb secondary interactions contribute significantly to the stability of the structure and to an increase in lattice energy of $[\text{Hg}(\text{CO})_2][\text{Sb}_2\text{F}_{11}]_2$ in the solid state.

In the demonstrated absence of π -back-bonding in $[\text{Hg}(\text{CO})_2]^{2+}$ (see preceding section), these OC–FSb contacts are, in our opinion, the principal reason that solid $[\text{Hg}(\text{CO})_2][\text{Sb}_2\text{F}_{11}]_2$ can be isolated and is found to exhibit thermal stability to 160 °C.

While *cis*-Pd(CO)₂(SO₃F)₂⁹ has been the first example where attention was drawn to the importance of secondary contacts in nonclassical carbonyls, we had at that time pointed to the peculiar packing in solid Au(CO)Cl,^{66a} which allows for weak Cl···CO contacts of ~3.35 Å, between adjacent linear molecules, slightly less than the sum of the van der Waals radii⁶³ of 3.4 Å. Very recently, we have determined the molecular structure of *mer*-Ir(CO)₃(SO₃F)₃^{66b} and have observed similar significant OC–OS interactions, comparable in strength to those found for *cis*-Pd(CO)₂(SO₃F)₂.

Our observation that almost all thermally stable nonclassical metal carbonyl salts have $[\text{Sb}_2\text{F}_{11}]^-$ as counteranion points to a unique role this anion can play, in stabilizing unusual cations via strong secondary, interionic contacts. The reason for this role of $[\text{Sb}_2\text{F}_{11}]^-$ will be discussed now.

(ii) Structural Comparison of $[\text{Hg}(\text{CO})_2][\text{Sb}_2\text{F}_{11}]_2$ to related compounds. A number of molecular structures^{67–76} have been reported previously, where the $[\text{Sb}_2\text{F}_{11}]^-$ anion is present together with molecular cations, formed by one or several main group elements.

The molecular cations in these compounds include the dihalogen I₂⁺,⁶⁷ the fluorocations TeF₃⁺,⁶⁸ IF₄⁺,⁶⁹ BrF₄⁺,⁷⁰ XeF₃⁺,⁷¹ and XeF₃⁺,⁷² and the halide derivatives SbCl₄⁺⁷³ and Se₂I₄²⁺.⁷⁴ In addition, examples have become known, where the anion–cation interaction involves hydrogen bonding. The fluoronium ions $[\text{H}_3\text{F}_2]^+$ and $[\text{H}_2\text{F}]^+$ are stabilized by H–F bonds to $[\text{Sb}_2\text{F}_{11}]^-$,⁷⁵ which in the first case forms a linear, symmetric bridge and an eclipsed configuration with retention of *D*_{4h} symmetry, while for $[\text{H}_2\text{F}][\text{Sb}_2\text{F}_{11}]$ a bridging angle of 144.2(3)° is reported for the anion in a preliminary publication. The oxonium ion $[\text{H}_3\text{O}]^+$ is found in $[\text{H}_3\text{O}][\text{Sb}_2\text{F}_{11}]$.⁷⁶ A very complicated structure is encountered that contains three crys-

(66) (a) Jones, P. G. *Z. Naturforsch.* **1982**, 37B, 823. (b) Wang, C.; Willner, H.; Batchelor, R. J.; Einstein, F. W. B.; Aubke, F. *Inorg. Chem.*, in press.

(67) Davies, C. J.; Gillespie, R. J.; Ireland, P. R.; Sowa, J. M. *Can. J. Chem.* **1974**, 52, 2048.

(68) Edwards, A. J.; Taylor, P. J. *Chem. Soc., Dalton Trans.* **1973**, 2150.

(69) Edwards, A. J.; Taylor, P. J. *Chem. Soc., Dalton Trans.* **1975**, 2174.

(70) Lind, M. D.; Christie, K. O. *Inorg. Chem.* **1972**, 11, 608.

(71) McKee, D. E.; Adams, C. J.; Zalkin, A.; Bartlett, N. *J. Chem. Soc., Chem. Commun.* **1973**, 26.

(72) McRae, V. M.; Peacock, R. D.; Russell, D. R. *J. Chem. Soc., Chem. Commun.* **1969**, 62.

(73) Miller, H. B.; Baird, H. W.; Bramlett, C. L.; Templeton, W. K. *J. Chem. Soc., Chem. Commun.* **1972**, 262.

(74) Nandana, W. A. S.; Passmore, J.; White, P. S.; Wong, C.-M. *Inorg. Chem.* **1990**, 29, 3529.

(75) Mootz, D.; Bartmann, K. *Angew. Chem., Int. Ed. Engl.* **1988**, 27, 391.

(76) Zhang, D. Ph.D. Thesis, University of British Columbia, 1995.

(63) Bondi, A. *J. Phys. Chem.* **1964**, 68, 441.

(64) Batchelor, R. J.; Einstein, F. W. B.; Gay, I. D.; Gu, J.-H.; Pinto, B. M. *J. Organomet. Chem.* **1991**, 411, 147.

(65) Subramanian, V.; Seff, K. *Acta Crystallogr.* **1980**, B36, 2132.

tallographically different $[\text{Sb}_2\text{F}_{11}]^-$ ions, all involved in interionic hydrogen bonding.

For the $[\text{Sb}_2\text{F}_{11}]^-$ anions, some consistent features emerge: The Sb–F_b–Sb bridge is within error limits symmetrical or at least very close to it. Bridging to the cation involves usually F atoms from the SbF₄ planes of the dioctahedral anion. The two planes are no longer eclipsed except for $[\text{BrF}_4][\text{Sb}_2\text{F}_{11}]$,⁷⁰ where D_{4h} symmetry seems to be retained; however, the structure determination is of low accuracy ($R = 0.14$). In addition, the SbF₄ planes are distorted and F₁SbF₆ angles are usually $\sim 85^\circ$, with displacement toward the bridging fluorine. Usually, a range of secondary contacts are formed. These interionic contacts are between 0.6 and 1.3 Å shorter than the sum of the van der Waals radii.⁶³ The shortest contact is found in $[\text{XeF}][\text{Sb}_2\text{F}_{11}]$ which, according to the authors, is best viewed as a molecular compound.⁷² There is some variation in the Sb–F_b–Sb bridge angle. One of the more acute angles is observed for $[\text{Hg}(\text{CO})_2][\text{Sb}_2\text{F}_{11}]_2$ with $147.6(3)^\circ$, comparable to angles found in $[\text{H}_3\text{O}][\text{Sb}_2\text{F}_{11}]$.⁷⁶ Hydrogen bonding may involve F atoms in the apical position of the $[\text{Sb}_2\text{F}_{11}]^-$ ion. As in $[\text{Hg}(\text{CO})_2][\text{Sb}_2\text{F}_{11}]_2$, where secondary contacts of two types, Hg–F and C–F, are found, in $[\text{Se}_2\text{I}_4][\text{Sb}_2\text{F}_{11}]_2$ both Se–F and I–F interionic interactions are reported.

These examples illustrate that the weakly nucleophilic, poorly coordinating, dinuclear $[\text{Sb}_2\text{F}_{11}]^-$ anion can engage in significant interionic contacts of varying strength. Due to these secondary interactions, the anion will distort. The important role $[\text{Sb}_2\text{F}_{11}]^-$ plays in stabilizing nonclassical carbonyl cations is evident from the report that in the thermally unstable salts $\text{Ag}(\text{CO})\text{B}(\text{OTeF}_5)_4$ ^{1,45} and $[\text{Ag}(\text{CO})_2][\text{B}(\text{OTeF}_5)_4]$,^{2,45} according to their low-temperature structures comparable C–F or C–O contacts of < 3.0 Å between ions are absent and only Ag–F contacts are reported.⁴⁵

In summary the $[\text{Sb}_2\text{F}_{11}]^-$ anion has been found to stabilize a number of unusual, highly electrophilic cations by secondary contacts. Such contacts may, as in the case of $\text{Se}_2\text{I}_4^{2+}$, involve two different acceptor sites on the cation. A similar observation is made for $[\text{Hg}(\text{CO})_2][\text{Sb}_2\text{F}_{11}]_2$ in this study, where Hg and C are acceptors.

The discussion will now turn to the cation $[\text{Hg}(\text{CO})_2]^{2+}$. There are four relevant precedents which allow a comparison. For the isoelectronic molecules or molecular ions $\text{Hg}(\text{CN})_2$ ²⁸ and $[\text{Au}(\text{CN})_2]^-$,⁷⁷ reliable molecular structures are reported. For the bis(carbonyl)gold(I) cation in $[\text{Au}(\text{CO})_2][\text{Sb}_2\text{F}_{11}]$,⁴ a detailed vibrational analysis including force field calculations has allowed the derivation of useful structural parameters. The fourth precedent is $[\text{Ag}(\text{CO})_2]^+$ with $[\text{B}(\text{OTeF}_5)_4]^-$ as counteranion. The compound is characterized by single crystal X-ray diffraction study at -100°C .^{2,45} The structure is complicated and contains three crystallographically different $[\text{Ag}(\text{CO})_2]^+$ cations.^{2,45} R_w is 10.2% and esd values are large (vide infra).

All five molecular species are depicted in Figure 6 in the form of idealized structural drawings. Included are the M–C and C–X (X = N or O) bond lengths, to allow a cross comparison between carbonyl and cyanide species. The valence force constants f_r (or $f(\text{C–X})$) and f_R (or $f(\text{M–C})$) are listed also where these are available.

All five species are essentially linear. Deviation from linearity is most pronounced for one of the $[\text{Ag}(\text{CO})_2]^+$ cations with a C–Ag–C angle of $169(1)^\circ$. Small deviations from linearity may be due to secondary contacts to the anion, as in

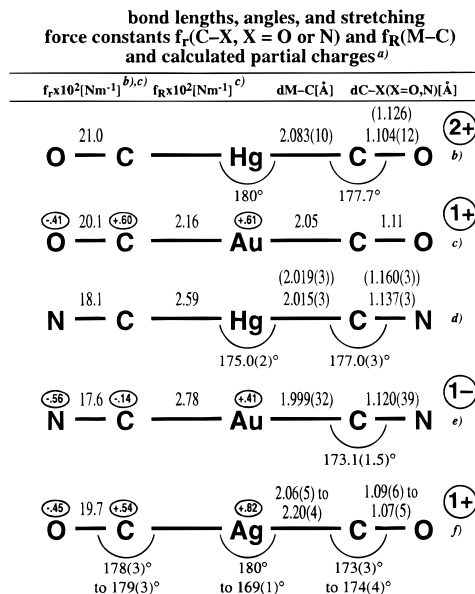


Figure 6. Structures of 5-atom linear carbonyls and cyanides of Ag(I), Au(I), and Hg(II): (a) ref 81; (b) this work; (c) ref 4; (d) ref 28b; (e) ref 77b; (f) refs 2 and 45.

$[\text{Hg}(\text{CO})_2][\text{Sb}_2\text{F}_{11}]_2$, to intermolecular association as in $(\text{Hg}(\text{CN})_2)$, or to counteraction effects for $[\text{Au}(\text{CN})_2]^-$, where weak coordination through nitrogen occurs. We have chosen salts with K^+ ,^{77a} Co^{2+} ,^{77b} and $[n\text{-Bu}_4\text{N}]^+$ ^{77c} as cations.

With $\bar{\nu}(\text{CO})$ and $\bar{\nu}(\text{CN})$ stretching vibrations at unusually high wavenumbers for all five molecules (see Table 3), initial attention is drawn to the C–O and C–N bond distances, which clearly rank at the lower (shorter) end of bond lengths reported for metal carbonyls and cyanides. Bond distances for C–O in $[\text{Ag}(\text{CO})_2]^+$ ^{2,46} are with 1.07(5)–1.09(6) Å the shortest values reported for metal carbonyls; however, the large esd values suggest caution. In addition, the bond length data are at variance with the observation of $\bar{\nu}(\text{CO})$ values for $[\text{Ag}(\text{CO})_2][\text{B}(\text{OTeF}_5)_4]$ at 2198 cm^{-1} .^{2,45}

For $[\text{Hg}(\text{CO})_2]^{2+}$, where $\bar{\nu}_{\text{av}}$ is with 2279.5 cm^{-1} the highest value reported so far, the shortest C–O bond distances are expected. The bond length of 1.104(12) observed does not differ significantly from 1.106(6) and 1.114(6) Å reported by us for the two CO groups in *cis*- $\text{Pd}(\text{CO})_2(\text{SO}_3\text{F})_2$ ⁹ where $\bar{\nu}_{\text{av}}(\text{CO}) = 2218\text{ cm}^{-1}$. Clearly, at these high CO bond orders of about 3, $\bar{\nu}(\text{CO})$ values are more sensitive to small changes in bond strength than are C–O bond distances. Furthermore, corrections for thermal motion of N or O atoms in the CN or CO ligands as they are applied to $\text{Hg}(\text{CN})_2$ ^{28b} and to $[\text{Hg}(\text{CO})_2]^{2+}$ generate bond distances of 1.160 and 1.126 Å, respectively, which are nearly undistinguishable from 1.1718 and 1.1281 Å for the CN radical⁷⁸ and CO,⁷⁸ respectively.

It seems more reasonable to use vibrational data and stretching force constants (see Table 3) when characterizing this group of compounds and when estimating the extent of π -back-donation. Where structural data are available, attention should focus on the M–C bond length instead, for four simple reasons. (i) The M–C bond distance is obviously very sensitive to changes in π -back-bonding; (ii) at M–C bond orders of about 1 or lower, differences in M–C bond distances are now clearly detectable and are not obscured by esd values; (iii) as found for $[\text{Hg}(\text{CO})_2]^{2+}$, thermal motion corrections are not necessary, where secondary contacts to C are found; and (iv) a comparison to a

(77) (a) Rosenzweig, A.; Cromer, D. T. *Acta Crystallogr.* **1959**, *12*, 709. (b) Zyontz, L. E.; Abraham, S. C.; Bernstein, J. L. *Acta Crystallogr. A* **1981**, *37*, 154. (c) Schubert, R. J.; Range, K. Y. *Z. Naturforsch.* **1990**, *45B*, 1118.

(78) Herzberg, G. *Spectra of Diatomic Molecules*, 2nd ed.; Van Nostrand: Toronto, 1966; pp 521 and 522.

wider body of structural data for related compounds with M–C bonds is now possible.

Of course, M–C bond distances will be metal dependent, but within this small homogeneous group of metals discussed here, variations in metal radii are expected to be small. It is difficult, however, to find a consistent set of radii, except perhaps the tetrahedral covalent radii, listed by Pauling.⁷⁹ They range from 1.53 (Ag) over 1.50 (Au) to 1.48 (Hg) Å. Alternatively, f_R values which are accurately known for $[\text{Au}(\text{CO})_2]^+$,⁴ $[\text{Au}(\text{CN})_2]^-$,⁵⁹ and $\text{Hg}(\text{CN})_2$ ⁵⁸ become useful and merit inclusion where structural data are not reliable or not known.

As seen in Figure 6, M–C distances in $[\text{Ag}(\text{CO})_2][\text{B}(\text{OTeF}_5)_4]$ vary over a wide range (2.06(5)–2.20(4) Å)^{2,45} and are difficult to interpret on account of their large esd values. For the remaining four molecular species, an interesting trend emerges. Based on both $d(\text{M}–\text{C})$ values and f_R data, the M–C bond strength decreases gradually in the order $[\text{Au}(\text{CN})_2]^- > \text{Hg}(\text{CN})_2 > [\text{Au}(\text{CO})_2]^+ > [\text{Hg}(\text{CO})_2]^{2+}$. Exactly the opposite trend is found for f_r and $\bar{\nu}(\text{CX})$ (X = N or O) for the four species. It appears logical to us that the two opposing trends in M–C and C–X bond length are best explained by gradually diminishing contributions from π -back-bonding to the M–C bond as the complex charge changes from –1 to +2.

In $[\text{Hg}(\text{CO})_2]^{2+}$, π -back-donation appears to reach a minimum. This is evident from a long Hg–C bond of 2.083(10) Å and as discussed above, from the highest f_r and $\bar{\nu}(\text{CO})$ values so far reported. Similar or shorter Hg–C bonds are found for isoelectronic $\text{Hg}(\text{CN})_2$ (2.015(3) Å),^{28b} CH_3HgCl ⁸⁰ (2.062 (20)), and CH_3HgBr (2.074(14)),⁸⁰ to list just a few, and it is reasonable to view the Hg–C bond in $[\text{Hg}(\text{CO})_2]^{2+}$, as well as in CH_3HgX (X = Cl or Br),⁸¹ as a pure σ -bond. Bond formation would involve donation from the 5σ molecular orbital on CO to a suitable σ symmetry orbital on Hg. This should necessarily result in a juxtaposition of positive charges of the type $\text{Hg}^{\delta+}–\text{C}^{\delta+}–\text{O}^{\delta-}$. This proposal is consistent with calculated charge distributions⁸¹ for linear $[\text{M}(\text{CO})_2]^+$ and $[\text{M}(\text{CN})_2]^-$, M = Ag or Au. As found for $[\text{Hg}(\text{CO})_2]^{2+}$, both the metal and the electrophilic C atom now become suitable acceptor sites for secondary contacts which will in part reduce the positive charges on Hg and C.

The proposed partial charge distribution for the Hg–C–O moieties of the cation explains both the weak and long Hg–C bond and the short and strong C–O bond, best illustrated by the unprecedentedly high $\bar{\nu}(\text{C}–\text{O})$ values. Both σ -donation from the slightly antibonding 5σ orbital on CO and polar contribution to the CO bond in our opinion are responsible for the high C–O bond strengths.

The molecular structure of $[\text{Hg}(\text{CO})_2][\text{Sb}_2\text{F}_{11}]_2$ and structural comparisons, to various $[\text{Sb}_2\text{F}_{11}]^-$ derivatives with nonmetallic main group cations and to isoelectronic and/or isostructural carbonyl and cyanide species, have allowed a good insight into bonding of this compound. As found previously for *cis*-Pd(CO)₂(SO₃F)₂,⁹ *mer*-Ir(CO)₃(SO₃F)₃,^{66b} and quite possibly Au(CO)Cl,⁶⁶ evidence for the importance of secondary contacts, in this case of the OC–F–Sb type, to the thermodynamic stability in the solid state is obtained.

It has been pointed out^{59,82} that the best synthetic approach to thermally stable nonclassical carbonyl derivatives involves the generation of the corresponding cations in strong protonic acids

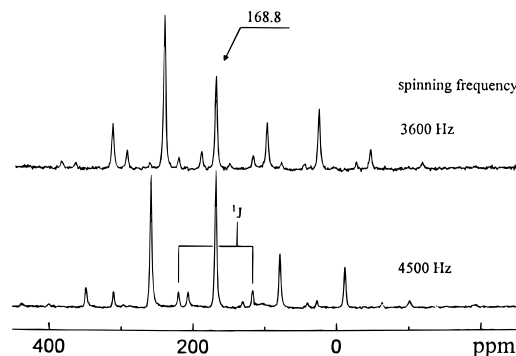


Figure 7. ^{13}C MAS-NMR spectrum of $[\text{Hg}(^{13}\text{CO})_2][\text{Sb}_2\text{F}_{11}]_2$ at two spinning frequencies, 3600 and 4500 Hz.

like $\text{HSO}_3\text{F}^{83}$ or superacids⁸⁴ like magic acid, $\text{HSO}_3\text{F}–\text{SbF}_5$, or SbF_5 itself. The proposed juxtaposition of positive charges in the sense $\text{M}^{\delta+}–\text{C}^{\delta+}$ explains why the metal–carbon bond will not be cleaved by protolysis in these highly acidic media. All these media are chemically not significantly different from the good secondary bond forming anions, SO_3F^- or $[\text{Sb}_2\text{F}_{11}]^-$, and it is suggested here that cation stabilization in solution involves OC–F–Sb or OC–F–OS solvation interactions, similar in essence to the secondary bonding effects in the solid state.

Along similar lines, Calderazzo and his students^{85–87} who have studied a number of nonclassical metal carbonyl halides, in particular chlorides of Pd(I), Pd(II), Pt(IV), Pt(II), and Au(I), have found thionyl chloride, SOCl_2 , to be an excellent solvent for chemical reactions, calorimetry, and vibrational spectroscopy. Thionyl chloride is a very poor donor solvent, which will not displace CO of the solutes. It seems to us that weak solvation by SOCl_2 on M and/or on C, of the type suggested to occur in HSO_3F or $\text{HSO}_3\text{F}–\text{SbF}_5$, is probable.

The bonding discussion has been very basic and qualitative. The nonclassical metal carbonyls have caught the interest of theoreticians.^{81,88} It is hoped that future efforts in this area will go beyond the molecular level.

(d) ^{13}C MAS-NMR Spectra. ^{13}C MAS-NMR spectra of isotopically enriched samples of both $[\text{Hg}(^{13}\text{CO})_2][\text{Sb}_2\text{F}_{11}]_2$ and $[\text{Hg}_2(^{13}\text{CO})_2][\text{Sb}_2\text{F}_{11}]_2$ are reported and discussed here, in order to complete the structural characterization of both materials. A brief summary of the results³⁰ is reported, and a comparison to related systems has been published.⁵⁹ Details on ^{13}C MAS-NMR spectra of silver(I), gold(I), and mercury(II) will be reported.⁸⁹

Data for $[\text{Hg}_2(^{13}\text{CO})_2][\text{Sb}_2\text{F}_{11}]_2$ are of poor quality for two reasons. (i) On account of the large molecular mass (mol wt 1364), the ^{13}C content is relatively low (1.9%), and error limits for our measurements are consequently large. (ii) Interference from $[\text{Hg}(^{13}\text{CO})_2][\text{Sb}_2\text{F}_{11}]_2$, formed by oxidation in subsequent preparations as discussed in the section on synthesis, presents an additional problem. Hence the discussion will center mainly on $[\text{Hg}(^{13}\text{CO})_2][\text{Sb}_2\text{F}_{11}]_2$.

The ^{13}C MAS-NMR spectrum of $[\text{Hg}(^{13}\text{CO})_2][\text{Sb}_2\text{F}_{11}]_2$ is shown in Figure 7. For $[\text{Hg}(\text{CO})_2][\text{Sb}_2\text{F}_{11}]_2$ $^1J(^{13}\text{C}–^{199}\text{Hg})$ is

(83) (a) Thompson, R. C. In *Inorganic Sulphur Chemistry*; Nickless, G., Ed.; Elsevier: Amsterdam, The Netherlands, 1968; p 81. (b) Gillespie, R. J. *Acc. Chem. Res.* **1968**, *1*, 202.

(84) Olah, G.; Prakash, S. G. K.; Sommer, J. *Superacids*; Wiley: New York, NY, 1985.

(85) Calderazzo, F. *Pure Appl. Chem.* **1978**, *50*, 49.

(86) Calderazzo, F.; Belli Dell'Amico, D. *Pure Appl. Chem.* **1986**, *58*, 561.

(87) Calderazzo, F. *J. Organomet. Chem.* **1990**, *400*, 303.

(88) Barnes, L. A.; Rosi, M.; Bauschlicher, C. W., Jr. *J. Chem. Phys.* **1990**, *93*, 609.

(89) Bodenbinder, M.; Balzer-Jöllenbeck, G.; Bley, B.; Willner, H.; Mistry, F.; Hägele, G.; Aubke, F. *Inorg. Chem.*, to be submitted.

(79) Pauling, L. *The Nature of the Chemical Bond*, 2nd ed.; Cornell University Press: London, 1948; p 179.

(80) Gordon, W.; Sheridan, J. J. *Chem. Phys.* **1954**, *22*, 92.

(81) Veldkamp, A.; Frenking, G. *Organometallics* **1993**, *12*, 4613.

(82) Aubke, F.; Wang, C. *Coord. Chem. Rev.* **1994**, *137*, 483.

found to be 5219 ± 5 Hz. The reduced coupling constant $K(^{13}\text{C}-^{199}\text{Hg})$ has a value of $96.94 \times 10^{21} \text{ N } \text{Å}^{-2} \text{ m}^{-3}$. The isotropic chemical shift is found to be 169 ppm, which is in agreement with previously reported values for nonclassical carbonyl derivatives.^{2,4,18a,46} The coupling constant $^1J(^{13}\text{C}-^{199}\text{Hg})$ is unprecedentedly high and exceeds the highest value previously reported for $\text{Hg}(\text{CN})_2$ in methanol solution^{29b} of 3142.5 Hz.

In magic acid ($\text{HSO}_3\text{F} + 2\text{SbF}_5$) a single line resonance at $\delta = 171.4(1)$ ppm is observed.

For solid $[\text{Hg}_2(\text{CO})_2][\text{Sb}_2\text{F}_{11}]$ an isotropic chemical shift of $\delta = 188.7(2)$ ppm is found. $^1J(^{13}\text{C}-^{199}\text{Hg})$ is with 3350(20) Hz very high, and $^2J(^{13}\text{C}-^{199}\text{Hg})$ is 850(50) Hz. The observed chemical shift of 188.7 ppm is unusual for a nonclassical carbonyl, slightly upfield from CO (184 ppm).

Summary and Conclusions

The synthesis, molecular structure, and spectroscopic characterization (IR, Raman, ^{13}C MAS-NMR) of bis(carbonyl)-mercury(II) undecafluorodiantimonate(V) $[\text{Hg}(\text{CO})_2][\text{Sb}_2\text{F}_{11}]_2$, the first thermally stable carbonyl derivative of a post-transition metal, are reported here. The synthesis is accomplished by the solvolysis of $\text{Hg}(\text{SO}_3\text{F})_2$ in liquid antimony(V) fluoride in a CO atmosphere at 100 °C. This method has been used initially to synthesize fluoroantimonate(V) salts containing main group cations like ClO_2^+ ,⁹⁰ I_2^+ ,⁴² Br_2^+ ,⁴² and $(\text{CH}_3)_2\text{Sn}^{2+}$.⁴³ The synthetic approach has been successfully adapted recently to the preparation of the first thermally stable noble metal carbonyl salts $[\text{Au}(\text{CO})_2][\text{Sb}_2\text{F}_{11}]_2$ ⁴ and $[\text{M}(\text{CO})_4][\text{Sb}_2\text{F}_{11}]_2$ ⁵ (M = Pd or Pt). More recently, $[\text{M}(\text{CO})_6][\text{Sb}_2\text{F}_{11}]_2$ (M = Ru or Os) has been added to this list.⁹¹

The molecular structure of $[\text{Hg}(\text{CO})_2][\text{Sb}_2\text{F}_{11}]_2$ shows a nearly linear $[\text{Hg}(\text{CO})_2]^{2+}$ cation with long Hg–C (2.083(10) Å) and

short (1.104(12) Å) CO bonds. More revealing are in our view significant secondary interionic OC–F–Sb contacts (2.653(9)–3.002(10)), which in the absence of π -back-bonding appear to strengthen the Hg–CO bond and contribute to the thermal stability of the compound to 160 °C.

As many examples from main group chemistry^{67–76} show, $[\text{Sb}_2\text{F}_{11}]^-$ is particularly well suited to engage in secondary bonding to electrophilic centers. All salts with noble metal carbonyl cations synthesized so far that show thermal stability well beyond 100 °C have $[\text{Sb}_2\text{F}_{11}]^-$ as anion.

The mercury–carbon bond in $[\text{Hg}(\text{CO})_2][\text{Sb}_2\text{F}_{11}]_2$ comes very close to a pure σ -bond, and many spectroscopic features of the cation, like $\bar{\nu}(\text{CO})_{\text{av}}$ at 2279.5 cm^{-1} , more than 135 cm^{-1} higher than in CO,¹⁸ the stretching force constant f_r of $21.0 \times 10^2 \text{ N m}^{-1}$, nearly identical with that of HCO^+ ($21.3 \times 10^2 \text{ N m}^{-1}$),⁴ and $^1J(^{13}\text{C}-^{199}\text{Hg})$ of 5219 Hz, are unprecedented in metal carbonyl and organo mercury chemistry.

Acknowledgment. Financial support by Deutsche Forschungsgemeinschaft (DFG), the Natural Science and Engineering Research Council of Canada (NSERC), and the North Atlantic Treaty Organization (NATO) is gratefully acknowledged. We thank Professor Steven H. Strauss, Colorado State University, for communicating his results to us prior to publication. Sheri Harbour is thanked for typing the manuscript.

Supporting Information Available: Additional crystallographic details, anisotropic thermal parameters, torsion angles, and interionic close contacts (6 pages). Ordering information is given on any current masthead page.

IC9507171

(90) Yeats, P. A.; Aubke, F. J. *J. Fluorine Chem.* **1974**, *4*, 343.

(91) Wang, C.; Bley, B.; Balzer-Jöllenebeck, G.; Lewis, A. R.; Sun, C. S.; Willner, H.; Aubke, F. *J. Chem. Soc., Chem. Commun.* **1995**, (in press).